JGR Atmospheres

RESEARCH ARTICLE
10.1029/2020JD033526

Evolution of Global Lightning in the Transition From Cold to Warm Phase Preceding Two Super El Niño Events

E. Williams[1], T. Bozóki[2,3], G. Sátori[2], C. Price[4], P. Steinbach[5,6], A. Guha[7], Y. Liu[1], C. D. Beggan[8], M. Neska[9], R. Boldi[10], and M. Atkinson[11]

[1]Parsons Laboratory of the Department of Civil and Environmental Engineering, Massachusetts Institute of Technology, Cambridge, MA, USA, [2]Geodetic and Geophysical Institute, Research Centre for Astronomy and Earth Sciences, MTA Centre for Excellence, Sopron, Hungary, [3]Doctoral School of Environmental Sciences, University of Szeged, Szeged, Hungary, [4]Department of Geophysics, Tel Aviv University, Tel Aviv, Israel, [5]Department of Geophysics and Space Science, Eötvös Loránd University, Budapest, Hungary, [6]MTA-ELTE Research Group for Geology, Geophysics and Space Science, Budapest, Hungary, [7]Centre for Lightning and Thunderstorm Studies, Department of Physics, Tripura University, Agartala, India, [8]British Geological Survey, Riccarton, Edinburgh, UK, [9]Institute of Geophysics, Polish Academy of Sciences, Warsaw, Poland, [10]College of Natural and Health Sciences, Zayed University, Dubai, United Arab Emirates, [11]HeartMath Institute, Boulder Creek, CA, USA

Key Points:

- Schumann resonance intensities are analyzed from distant stations in connection with two super El Niño events
- Increased Schumann resonance intensity indicates enhanced lightning activity in the transition from cold to warm phase in both events
- Schumann resonance intensity may be a precursor for occurrence of super El Niño events and for maxima in global surface air temperature

Correspondence to:
T. Bozóki,
bozoki.tamas@csfk.org

Citation:
Williams, E., Bozóki, T., Sátori, G., Price, C., Steinbach, P., Guha, A., et al. (2021). Evolution of global lightning in the transition from cold to warm phase preceding two super El Niño events. *Journal of Geophysical Research: Atmospheres*, *126*, e2020JD033526. https://doi.org/10.1029/2020JD033526

Received 16 JUL 2020
Accepted 26 OCT 2020

Abstract Multistation observations of Schumann resonance (SR) intensity document common behavior in the evolution of continental-scale lightning activity in two super El Niño events, occurring in 1997/98 and 2015/16. The vertical electric field component of SR at Nagycenk, Hungary and the two horizontal magnetic field components in Rhode Island, USA in 1997, and in 2014–2015, the two horizontal magnetic field components at Hornsund, Svalbard and Eskdalemuir, United Kingdom as well as in Boulder Creek, California and Alberta, Canada exhibit considerable increases in SR intensity from some tens of percent up to a few hundred percents in the transition months preceding the two super El Niño events. The UT time distribution of anomalies in SR intensity indicates that in 1997 the lightning activity increases mainly in Southeast Asia, the Maritime Continent and India, i.e. the Asian chimney region. On the other hand, a global response in lightning is indicated by the anomalies in SR intensity in 2014 and 2015. SR-based results are strengthened by comparison to independent lightning observations from the Optical Transient Detector and the World Wide Lightning Location Network, which also exhibit increased lightning activity in the transition months. The increased lightning is attributable to increased instability due to thermodynamic disequilibrium between the surface and the midtroposphere during the transition. The main conclusion is that variations in SR intensity may act as a precursor for the occurrence and magnitude of these extreme climate events, and in keeping with earlier findings, as a precursor to maxima in global surface air temperature.

Plain Language Summary Schumann resonance (SR) is a global phenomenon produced by low frequency electromagnetic radiation (<100 Hz) from worldwide lightning. Lightning strokes act as wideband electromagnetic antennas transmitting in this specific frequency band, and due to the extreme low attenuation of electromagnetic waves, their radiated signals can be observed anywhere on Earth. This phenomenon enables the monitoring of global lightning with just a very few (up to four in this study) observation sites around the globe. The main advantage of the SR-based method is the expectation that all of the worldwide lightning contributes to the measured SR field, which means the absence of detection efficiency problems which are inherent with many other lightning detection methods.

In this work, we use SR measurements to monitor changes in both regional and global lightning activity in connection with two extremely large magnitude, so called "super" El Niño events (1997/98 and 2015/16). Our conclusion is that SR intensity variations in the transition months preceding these two El Niño events indicate an important increase in lightning activity attributable to thermodynamic disequilibrium. We suggest that SR intensity variations might be applied in the future to predict the occurrence of these extreme climate events.

1. Introduction

The El Niño–Southern Oscillation (ENSO) is an irregularly repeating interannual variation with alternations between a cold (La Niña) phase and a warm (El Niño) phase, as measured in sea surface temperature (SST). Both ENSO episodes have worldwide influence on the global climate but the warm El Niño period can cause more dramatic changes, manifest in heavy rainfall or severe drought, mainly in the tropical and subtropical regions (Allen et al., 1996). A challenging and up-to-now unresolved issue is the prediction of occurrence and magnitude of El Niño episodes. As with the effects of ENSO, the main global lightning activity worldwide can also be found in the tropics, in three dominant continental regions known as the lightning "chimneys": the Maritime Continent (MC) together with the Indian subcontinent, Africa (including the Congo Basin) and the Americas (including the Amazon Basin of South America). The World Meteorological Organization (WMO) recently declared lightning as one of the essential climate variables (Aich et al., 2018) which underlines the importance of lightning research in studying the impact of ENSO on global climate (and see further references below).

Several studies have looked at the ENSO phenomenon with a focus on its possible effect on lightning activity in selected regions and with emphasis on distinguishing the behavior in the warm phase and the cold phase (see further discussion in Section 4.2). For example, the flash rate was higher over the MC in the peak warm phase of March 1998 than during the following cold episode in March 1999 of the super El Niño of 1997/98 (Hamid et al., 2001). Comparison of lightning activity in the El Niño (2002) and La Niña years (1998–2001) showed that lightning activity over India increased by nearly 18% in the seasonally matched warm period (Kandalgaonkar et al., 2003). Evidence for increased lightning activity in the Indian subcontinent and Southeast Asia during the El Niño phase was confirmed by several other works as well (e.g., Ahmad & Ghosh, 2017; Kumar & Kamra, 2012; Tinmaker et al., 2017; Yoshida et al., 2007; Yuan et al., 2016). Analysis of seasonal rainfall and lightning activity showed a strong correlation with ENSO episodes over the central and eastern Mediterranean Sea (Price & Federmesser, 2006). The increased wintertime Southeastern U.S. lightning (thunderstorm) activity during 1997–1998 was attributed to the enhanced synoptic-scale forcing associated with ENSO (Goodman et al., 2000). Global lightning has also been examined from an ENSO perspective by Chronis et al. (2008) and Sátori et al. (2009). Dowdy (2016) has suggested the potential for seasonal forecasting of lightning and thunderstorm activity in various regions throughout the world by studying large-scale modes of atmospheric and oceanic variability. According to his results, ENSO has the strongest relationship with lightning activity during each individual season.

Schumann resonances (SR) are the global electromagnetic resonances of the Earth-ionosphere cavity maintained by the electromagnetic radiation (<100 Hz) of the worldwide lightning activity (Schumann, 1952). A comprehensible summary of SR can be found in Price (2016) while for a more extensive picture one may consult Nickolaenko and Hayakawa (2002, 2014). In early ENSO/lightning studies, Williams (1992) found a close correlation between the surface temperature anomaly (Hansen & Lebedeff, 1987) and the horizontal magnetic field component of SR observed at West Greenwich, Rhode Island (RID) in the period 1969–1974, spanning two warm and two cold ENSO episodes. The meridional redistribution of global lightning was deduced from SR frequency variations during the super El Niño event of 1997/98 (Sátori et al., 1999). Later, independent evidence for the meridional as well as zonal redistribution of global lightning was given for the super El Niño event of 1997/98 and a moderate El Niño episode in 2002/03 based on Optical Transient Detector (OTD)/Lightning Imaging Sensor (LIS) satellite observations (Sátori et al., 2009). It was also shown that the global lightning activity tends to increase worldwide during warm ENSO events over land, especially in the MC and India (Sátori et al., 2009). Beggan et al. (2019) studied the possible relationship between SR and Madden Julian Oscillation (MJO) in 2013–2018. They have found that the periodical variations of SR spectral parameters (intensity, frequency) and MJO are occasionally in phase but exclusively in the years under La Niña condition before and after the super El Niño of 2015/16. In general, the recording of SR at a few distant stations is known to be an efficient tool to monitor global lightning without the problems of detection efficiency inherent with other lightning detection methods (Boccippio et al., 2000; Hutchins et al., 2012; Said et al., 2010).

Up to now the great majority of studies addressing the ENSO-lightning relationship have dealt with the general behavior of lightning activity during the ENSO warm and cold episodes, respectively. One notable exception is Guha et al. (2017) who studied the warm-to-cold ENSO transition in 2009/2010. Few studies

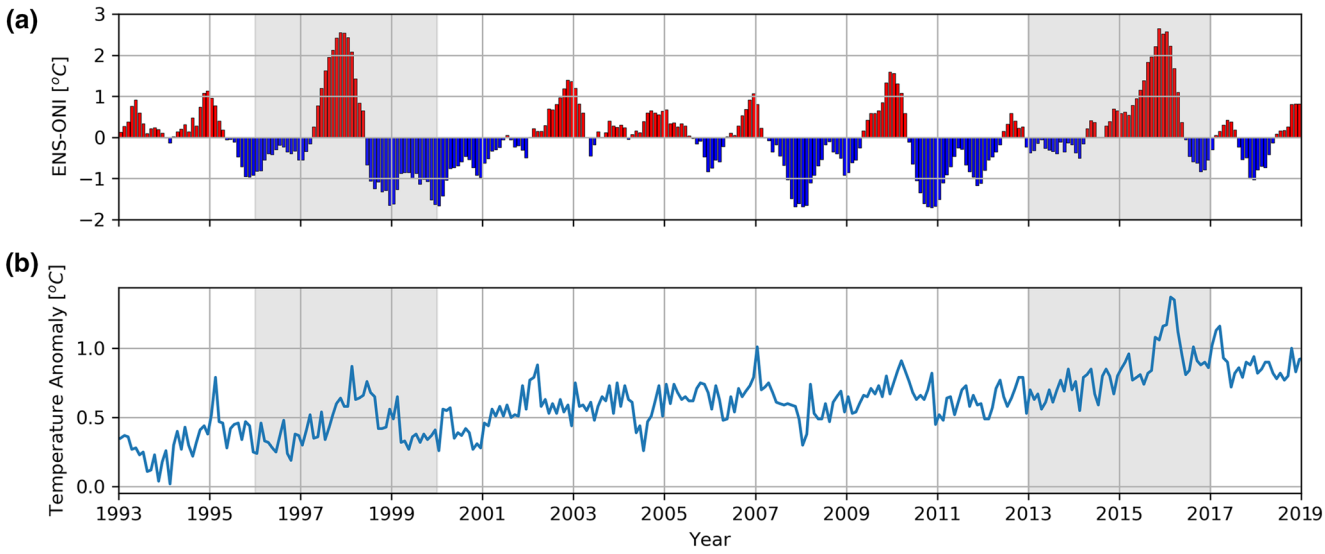

Figure 1. (a) The Ensemble Oceanic NINO Index (ENS-ONI) and (b) the global monthly mean surface temperature change in the time period of 1993–2019. Gray-shade background highlights the super El Niño time periods 1996–1999 and 2013–2016 investigated in this study. In the upper plot warm (El Niño) periods are shown in red and cold (La Niña) periods are shown in blue.

have focused on the temporal evolution of continental-scale lightning activity on the ENSO timescale. The transition period from peak cold phase to peak warm phase comprises many months and occasionally more than one year. In this work we study global lightning on a monthly basis in the time period of two super El Niño events in 1997/98 and 2015/16 based on SR observations. Although these two extreme climate events were markedly different in some important aspects (L. Chen et al., 2017), we aim to reveal common signatures in their evolution with attention focused on their effect on continental-scale lightning activity. We shall also be concerned with the precursory signature of ENSO lightning on the global temperature, given earlier evidence that heat is transferred from the ocean to the tropical atmosphere in the warm phase, and subsequently transferred to the global atmosphere (Trenberth et al., 2002). These findings will hopefully contribute to the better understanding and predictability of ENSO in the future.

2. Data and Methods

For our analyses we have selected the two strongest El Niño events of the last quarter century, in 1997/98 and in 2015/16, which are often called "super" El Niño events (Hansen et al., 2018, https://www.webber-weather.com/ensemble-oceanic-nino-index.html) due to their extraordinary large magnitude (Figure 1). From the numerous different indices characterizing the ENSO phenomenon, the Ensemble Oceanic NINO Index (ENS-ONI) has been selected which is an observation-based and real-time index given with monthly time resolution. The ENS-ONI index is determined by averaging SST anomalies in an area of the east-central equatorial Pacific Ocean (Nino-3.4 region).

The global context of the tropical ENS-ONI index in Figure 1 is shown by the comparison of the record of global monthly mean surface temperature change from NASA (https://data.giss.nasa.gov/gistemp/graphs_v4/) on the same time scale. This record is included here to show a well-known result that El Niño events transfer heat from the ocean to the atmosphere (Trenberth et al., 2002), a process that ultimately warms the global atmosphere. Accordingly, the peak El Niño times in Figure 1 lead the maxima in global air temperature by times of order 2–3 months, with the largest peak temperatures linked with the two extreme events.

At the Nagycenk Geophysical Observatory (NCK, 47.6°N, 16.7°E) (also known as Széchenyi István Geophysical Observatory) in Hungary the continuous recording of the SR spectral parameters corresponding to the vertical electric field began in May 1993 (Bór et al., 2020; Sátori et al., 1996, 2013). The applied complex demodulation algorithm provides the frequency and the amplitude of the first three SR modes (Sátori

et al., 1996). Time periods with unrealistic spectral parameters, e.g., due to local weather conditions, were removed manually. We utilize this data set over the 4-year-long time period of 1996–1999 to investigate the evolution of the super El Niño event of 1997/98. Two-component magnetic observations at MIT's Schumann resonance station in West Greenwich (RID, 41.6°N, 71.7°W) are also used in case of this super El Niño event. Modal parameters for the SR at RID are extracted from spectral intensity by Lorentzian fitting (Boldi et al., 2018; Mushtak & Williams, 2002).

Magnetic SR measurements at Hornsund (HRN, 77.0°N, 15.6°E), Eskdalemuir (ESK, 55.3°N, 3.2°W), Alberta (ALB, 51.9°N, 111.5°W) and Boulder Creek (BOU, 37.2°N, 122.1°W) stations were processed in the 4-year time period of 2013–2016 to investigate the evolution of the super El Niño event of 2015/16. The HRN station is operated by the Polish Academy of Sciences at Svalbard, the ESK station by the British Geological Survey in the UK, and the ALB and BOU stations by the HeartMath Institute (https://www.heartmath.org/gci/) in the United States and in Canada, respectively. These sites are equipped with a pair of induction coil magnetometers aligned with the geographical north-south direction (H_{NS}) and perpendicular to it (H_{EW}). The measurements were bandpass-filtered and 10 min-average spectra were generated for the two magnetic components separately. The weighted average method as in Musur and Beggan (2019) was applied to obtain the SR spectral parameters (intensity and frequency). Time periods with unrealistic spectral parameters were manually removed from the data set. The SR data from the HRN station are not available between September 2015 and March 2016 due to technical reasons.

In this study we calculate the monthly average diurnal variation of the first SR mode's intensity (I_1) with 10 min time resolution, i.e., a (12 × 144) matrix characterizes each processed year (the 10 min time resolution yields 6 × 24 = 144 intensity values for each of the 12 months within a year). The main advantage of this approach is that in addition to highlighting the months with unusual SR intensity it provides the UT time characteristics of the anomaly as well, which has crucial importance in the interpretation of the results. In order to reveal possible ENSO-related variations in I_1 (12, 144) it is necessary to remove the substantial seasonal variation (see e.g., Sátori, 1996) from the data. Therefore, we introduced a normalization process as follows:

$$I_{1,norm}\left[\%\right] = 100\% \cdot \frac{I_1 - I_{1,av}}{I_{1,av}},$$

where $I_{1,av}$ (12, 144) denotes the 4-year average of I_1 (12, 144) (1996–1999 or 2013–2016). In practice, this means that the average value for all the months of e.g., January is removed from each of the four years to leave the residual value. Hereafter, we call this quantity "normalized SR intensity."

A rich archive of thermodynamic soundings is maintained by the University of Wyoming (http://weather.uwyo.edu/upperair/sounding.html) that have been used to explore the thermodynamic origins of the ENSO-related lightning variations. Convective available potential energy (CAPE) sets an upper bound on the updraft speeds that can be achieved in thunderstorm convection (Williams & Stanfill, 2002), and these updraft speeds sensitively influence the ice-based microphysics that controls charge separation and lightning. Values of CAPE are also provided on the UWYO site, as well as the vertical profiles of cloud buoyancy that are helpful in diagnosing the changes in convective adjustment to surface warming that characterize the cold to warm transition in ENSO. CAPE is calculated by the pseudo-adiabatic process and with air parcels with a wet bulb potential temperature averaged over the lowest 500 m of the sounding.

In order to support our SR-based results and to reveal the origin of the observed anomalies in SR intensity, selected months of the two investigated time periods are analyzed based on independent data sets of lightning observations as well. Monthly averages of the 2.5° × 2.5° gridded flash number density (flash/km^2) data provided by the OTD satellite (Cecil et al., 2014) are applied for the time period of the super El Niño event of 1997/98 (neither OTD nor LIS data were available for the second event). In addition, monthly averages of 1° × 1° gridded World Wide Lightning Location Network (WWLLN, http://wwlln.net) flash rate (flash/1° × 1°) data, based on very low frequency (VLF) observations, are analyzed for the super El Niño event of 2015/16 (WWLLN data were not available for the first event).

3. Results

The interpretation of Schumann resonance intensities as a global lightning indicator is not immediately straightforward to nonspecialists in meteorology and climate studies, and so some discussion on this aspect is appropriate in advance of the presentation of the results themselves. To interpret the SR-based results to be shown in Figures 2–4 it is important to be aware of the characteristic diurnal variation of SR intensity which is strongly coupled to the diurnal variation of global lightning activity. The major part of global lightning is concentrated in the tropical continental regions, which can be divided into three main areas: the African, the American, and the Asian lightning "chimneys" (Christian et al., 2003). As the most intense time period of lightning activity corresponds to the afternoon hours in local time (Williams et al., 2000), the activation of the main lightning chimneys occurs separately in universal time. The maximum SR intensity corresponding to the Asian, the African, and the American chimneys are usually at around 8, 15, and 20 UT, respectively. This property of lightning activity is mirrored by the diurnal variation of SR intensity and makes it possible to distinguish the contribution of the different chimneys to the observed increase in SR intensity. It is important to note that an electric antenna is isotropic in its response and so for all wave propagation directions. In contrast, the magnetic coils are most responsive to electromagnetic waves propagating perpendicular to their orientation, and thereby they yield additional information about the direction of lightning activity connected to the observed anomalies in SR intensity.

3.1. Results Based on SR Measurements

Figure 2a shows the ENS-ONI index and Figure 2b presents the normalized SR intensity variation of the E_Z field component at the NCK station between 1996 and 1999, a 4-year time period corresponding to the super El Niño event of 1997/98. The most conspicuous intensification in the normalized intensity of SR occurs in February (∼70%) and in April (∼90%), clearly in the transition of ENSO from the La Niña to its El Niño phase (Figure 2a). The intensification is not uniform in UT time but maximizes near 10–14 UT (Figure 2b) when the lightning in the Indo-Gangetic Plain in northern India is most active, a region previously highlighted for exceptional lightning activity (Albrecht, 2016; Cecil et al., 2014; Guha et al., 2017; Kandalgaonkar et al., 2005). In contrast, only minor intensification is evident during the warm phase in the normalized SR intensity which is more evident in November and December 1997 in Figure 2b where the yellow colors replace the light blue ones. Later on, a notable suppression of activity is evident during the declining period of the warm phase (January, February, March, and April of 1998). The world maps show the location of the two distant SR stations: NCK (Figure 2c) and RID (Figures 2d and 2e). The vertical electric field component (E_Z) was measured at NCK and the two horizontal magnetic field components (H_{NS} and H_{EW}) were recorded in RID. The E_Z antenna is responsive to any direction while the induction coils are the most sensitive for the great propagational circle path perpendicular for the coil axis. The orange and green lines in the maps (Figures 2d and 2e) indicate those directions. Diurnal variations of the first SR mode's intensity in April 1997 (red) are compared with April 1996 (blue) for the E_Z field component at NCK (Figure 2h), for the H_{EW} (Figure 2g) component, as well as for the H_{NS} (Figure 2h) magnetic field components at RID, respectively. The SR intensity exhibits considerable increase in the E_Z field component at NCK between 06 and 16 UT with maximum intensity at 11 UT in April 1997 (Figure 2f). The H_{EW} field component shows increased intensity at RID between 10 and 15 UT while the intensity of the H_{NS} field component shows little change between April 1996 and April 1997. On the basis that the H_{NS} field component (responsive to the African lightning activity at RID, see Figure 2h), shows little change between April 1996 and April 1997, we can conclude that the increased SR intensity in the E_Z field component at NCK and in the H_{EW} field component in RID are attributable to the increased lightning activity in the MC and in India. That country has been shown to have the maximum lightning activity near 11 UT with a sustained period of decay thereafter (Chaudhari et al., 2010). The big difference between the SR response in E_Z at NCK and in H_{EW} in RID may be explained by the fact that the DC component of the electric field is not perfectly separated from the AC component (SR) in the electronics of the preamplifier in case of large changes in the static field ($\gtrsim$300 V/m). Both SR and potential gradient measurements have been running in parallel at NCK (Bór et al., 2020) and the occasional contamination of SR intensity with anomalously increased PG values was demonstrated by Märcz et al. (1997). As was shown by Märcz and Sátori (2005) the PG measurement at NCK was also responsive to the super El Niño of 1997/98. Therefore, a likely scenario is that the SR observations mirror

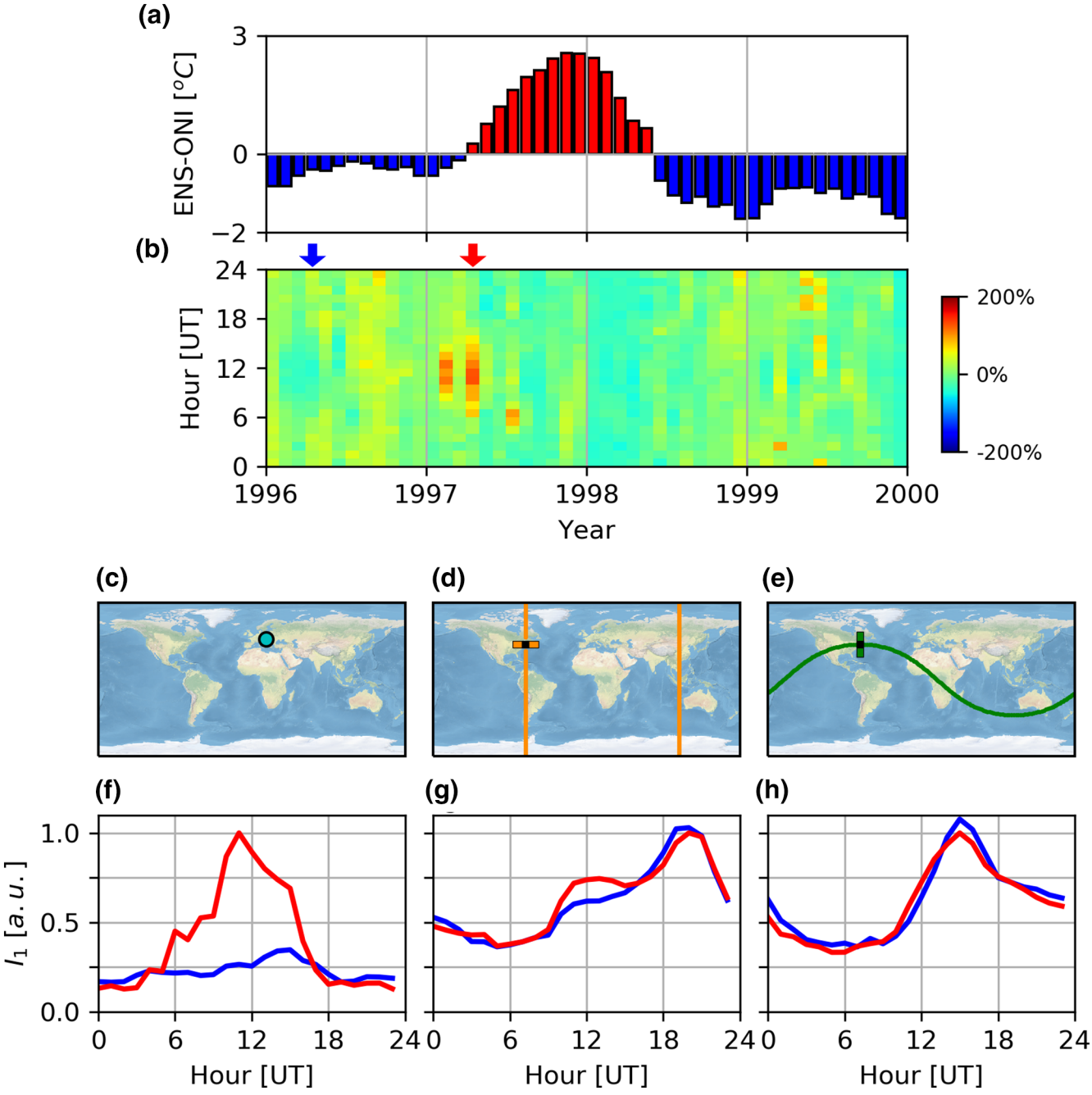

Figure 2. SR-based observations for the super El Niño event of 1997/98. (a) The ENS-ONI index and (b) the normalized Schumann resonance (SR) intensity at Nagycenk (NCK) station between 1996 and 1999. The color scale represents the bipolar % deviations from the monthly/seasonal means of absolute intensity based on the 4-year period of Schumann resonance observations (see the Data and Methods section for more details). April 1996 and April 1997 are marked with a blue and a red arrow, respectively. (c–e) Maps with the locations of (c) NCK (for Ez) and (d and e) RID (for H_{NS} and H_{EW}) stations. Panels (d and e) show the orientation of the magnetic coils (H_{NS} = green; H_{EW} = orange) and the propagation directions for which they are the most sensitive. (f–h) Diurnal variations of the first SR mode's intensity in April 1997 (red) as compared with April 1996 (blue) (f) for the Ez field component at NCK, (g) for the H_{EW} as well as (h) for the H_{NS} magnetic field components at RID, respectively. The diurnal variations in intensity in (f–h) are all normalized to unity for the maximum value in April 1997.

both the variation in the AC (SR) and the DC field connected with the super El Niño event of 1997/98 which enlarges the observed intensity in the first SR mode at NCK compared to the magnetic measurement at RID. This idea is supported by the observation that the percentage increase at the maximum of the mean diurnal

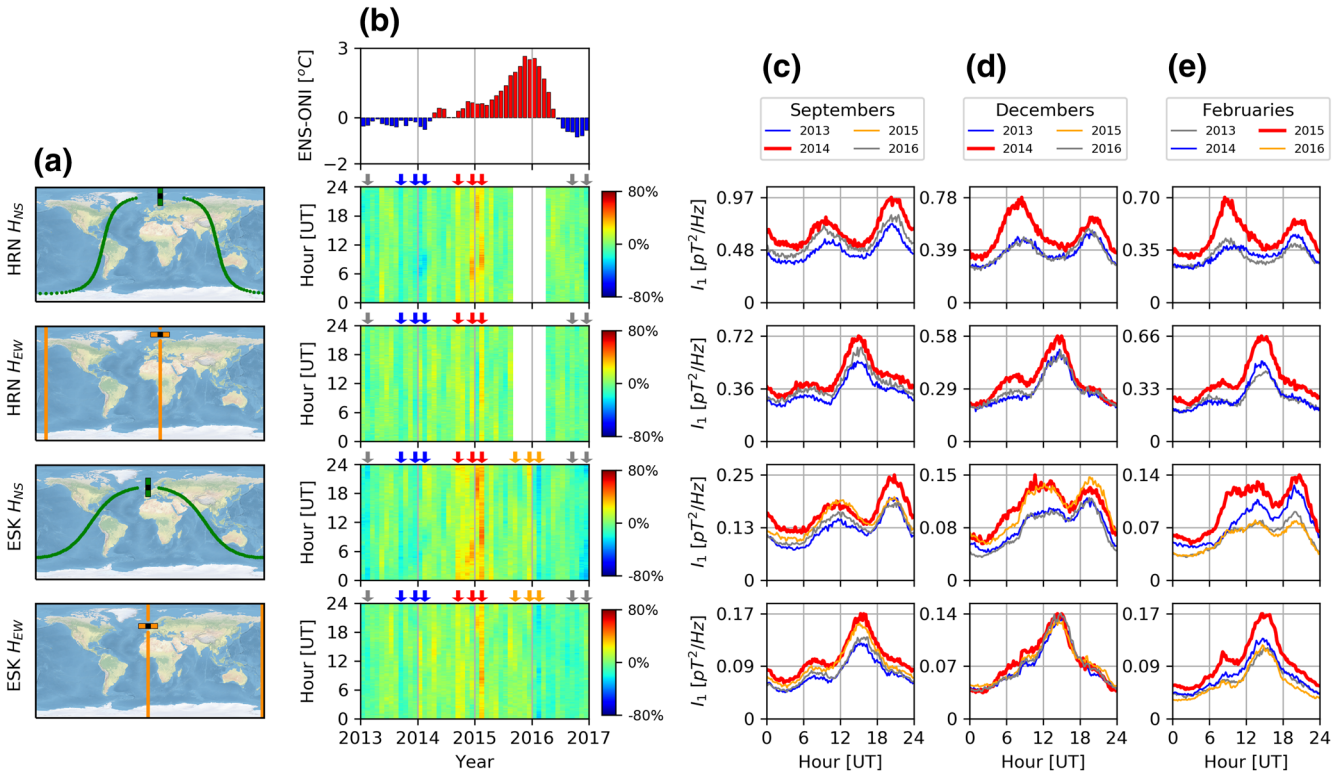

Figure 3. SR intensity at Hornsund (HRN) and Eskdalemuir (ESK) stations over the period 2013–2017. (a) Maps with the locations of the SR stations, the orientation of the magnetic coils (H_{NS} = green; H_{EW} = orange) and the propagation directions for which they are the most sensitive. (b) The ENS-ONI index (top) and the normalized SR intensity plots. The color scale represents the bipolar % deviations from the monthly/seasonal means of absolute intensity based on the 4-year period (see the Data and Methods section for more details). (c–e) Diurnal variations of the first SR mode's intensity in pT^2/Hz for the two magnetic field components at the two stations (four panels in each column) in selected months: (c) Septembers, (d) Decembers, and (e) Februaries. The red curves in the panels of column (c) indicate September 2014, panels of column (d) December 2014 and panels of column (e) February 2015 (all are transition months indicated with red arrows in column b). (c) The orange curves refer to September 2015, (d) December 2015, and (e) February 2016 (all are in the main phase of the super El Niño of 2015/2016 indicated with orange arrows in the ESK-related portion of column b). The blue curves indicate (c) September 2013, (d) December 2013, and (e) February 2014 (all are in cold or neutral phase preceding the super El Niño of 2015/16 indicated with blue arrows in column b). The gray curves refer to (c) September 2016 and (d) December 2016 as well as (e) February 2013.

intensity variation between April 1996 and April 1997 is smaller in the second (~300%) and third (~250%) SR modes than in the first mode (~350%) at NCK (not presented here). In addition, the sunrise time at RID is near 10 UT and the SR intensity is diminished under nighttime condition before 10 UT due to the day-night asymmetry of the Earth-ionosphere cavity (Sátori et al., 2007, 2016). The NCK station as well as the India and MC source regions are under daytime condition during the maximum lightning activity in those regions in April.

Figures 3 and 4 present the results for the super El Niño event of 2015/16. World maps are added to these figures to show the location of the widely separated SR stations: HRN, ESK (Figure 3a) and ALB, BOU (Figure 4a). The orientations of the magnetic coils and the propagation directions, for which the coils are the most sensitive, are also indicated. The H_{NS} and H_{EW} coils are marked consequently with green and orange colors, respectively. Figures 3b and 4b show the normalized SR intensity variations in the H_{NS} and H_{EW} magnetic field components between 2013 and 2016 while Figures 3c–3e and 4c–4e present the diurnal SR intensity variation of selected months from the same time period.

The 2015/16 super El Niño event showed a substantially longer duration than the 1997/98 event (26 vs. 14 months, see Figure 1). At the investigated stations the first remarkable SR intensification took place in September 2014, when the ENS-ONI index jumped from a near zero to a markedly positive value (Figures 3b and 4b). The largest SR intensifications appear in the period December 2014–February 2015, when after a small decrease the ENS-ONI index starts to increase strongly again. This time period can be regarded

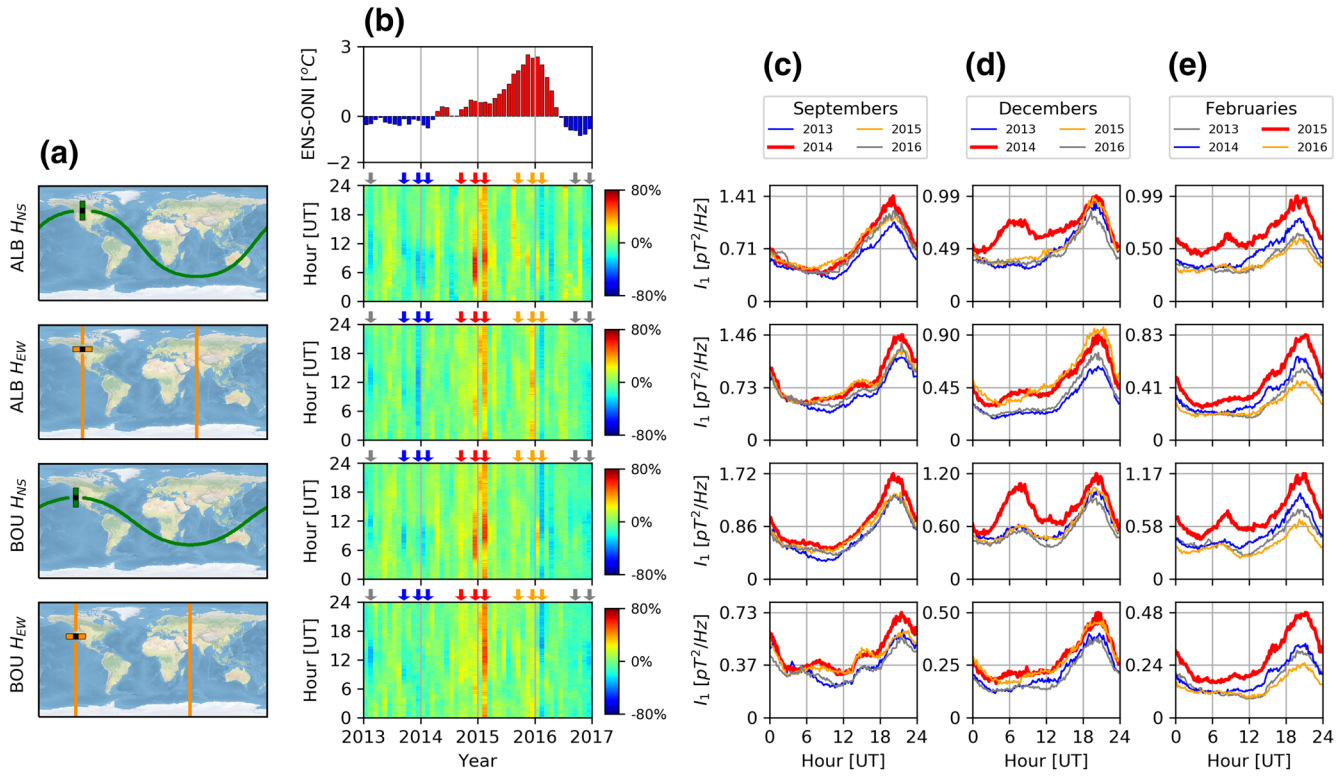

Figure 4. SR intensity at Alberta (ALB) and Boulder Creek (BOU) stations over the period 2013–2017. (a) Maps with the locations of the SR stations, the orientation of the magnetic coils (H_{NS} = green; H_{EW} = orange) and the propagation directions for which they are the most sensitive. (b) The ENS-ONI index (top) and the normalized SR intensity plots. The color scale represents the bipolar % deviations from the monthly/seasonal means of absolute intensity based on the 4-year period (see Data and Methods section for more details). (c–e) Diurnal variations of the first mode's SR intensity in pT^2/Hz for the two magnetic field components at the two stations (four panels in each column) in selected months: (c) Septembers, (d) Decembers, and (e) Februaries. The red curves in the panels of column (c) indicate September 2014, panels of column (d) December 2014 and panels of column (e) February 2015 (all are transition months indicated with red arrows in column b). The orange curves refer to (c) September 2015, (d) December 2015, and (e) February 2016 (all are in the main phase of the super El Niño of 2015/16 indicated with orange arrows in column b). The blue curves indicate (c) September 2013, (d) December 2013, and (e) February 2014 (all are in the cold or neutral phase preceding the super El Niño of 2015/16 and indicated with blue arrows in column b). The gray curves refer to (c) September 2016 and (d) December 2016 as well as (e) February 2013.

as a second transition interval of the El Niño episode. The last transition month when conspicuous SR intensification is observed in the normalized SR intensity plots is April 2015.

Previous ENSO-lightning studies have focused on lightning enhancement in the peak El Niño (warm) phase rather than in the transition, and that bears checking for this case as well. Similar to the 1997/98 event, secondary SR intensification is evident near the maximum of the 2015/2016 super El Niño event. This can be seen in the September and December months of 2015 (yellow color) in the record from the ESK station in Figure 3b and also in the interval September to December 2015 (yellow color, a few tens of percent enhancement) in the records from the BOU and ALB stations in Figure 4b. A notable suppression of activity is evident during the declining period of the warm phase (February, March, and April of 2016) just as in the case of the 1997/98 event in Figure 2.

With a goal toward highlighting the interannual variations in SR signals, the diurnal variations of the first SR mode's intensity in the two magnetic field components at the four stations were selected in the same months (September, December, February) of four consecutive years, as shown for the HRN and ESK stations in Figures 3c–3e as well as for the ALB and BOU stations in Figures 4c–4e. Variation of SR intensity measured with two magnetic field components at four distant stations can capture the anomalous behavior of global lightning activity as the great circle paths shown in the maps cross one or more tropical chimney regions. The colored arrows in Figures 3b and 4b show the selected months for diurnal analysis from the 4-year time window. The red color identifies the months in the transition period preceding the super El

Niño of 2015/16, the orange color refers to the main phase of the super El Niño, the blue color represents the cold (neutral) period before the super El Niño event and the gray color indicates those months which are separated from the cold, transition, and main phase intervals but included in the 4-year normalization procedure. The diurnal SR intensities are greatest in the transition months (curves with red color) for all four SR stations and for both the H_{EW} and H_{NS} magnetic field components, as shown in Figures 3c–3e and 4c–4e. Consequently, a worldwide intensification of lightning activity occurred during the transition months. The diurnal SR intensity variations in the main phase of the super El Niño (curves with orange color) approached the level of SR intensities in the transition month of September and December (Figures 3c, 3d, 4c, and 4d) and before the peak of the super El Niño. In the later declining warm phase of the super El Niño, in February 2016 (Figures 3e and 4e), the SR intensity was greatly diminished. The level of diurnal SR intensity variations does decrease in the months of the cold period preceding the transition interval (curves with blue colors) and in the months at the beginning and end of the 4-year time window (curves with gray color). The great circle path at HRN and ESK in the case of the H_{NS} field component crosses the MC and West India (see Figure 3a). Large SR intensity anomalies are attributed to these regions in the transition months: December 2014 and February 2015 (corresponding to the red curves in Figures 3d and 3e). A huge increase (~80%–100%) of SR intensity in H_{NS} occurred at the HRN station near 8 UT when the MC shows the customary maximum lightning activity and an anomalously large increase of SR intensity appeared at the ESK station as well as a wide maximum centered near 12 UT when the Indian subcontinent shows the usual maximum lightning activity. The H_{EW} field component at HRN indicated a noticeable increase of lightning activity in the African chimney region at around 15 UT at both the HRN and ESK stations in the transition month of February 2015 (corresponding red curves in Figure 3e). The H_{NS} field component at ALB and BOU are responsive to the lightning activity in Australia and the southeastern part of the MC (see the great circle paths in the maps of Figure 4a). In the transition month of December 2014, a large increase (~100%–150%) of SR intensity was observed at these two stations near 7 UT, when these regions show the maximum lightning activity (corresponding red curves in Figure 4d). A smaller response in SR intensity can be seen in February 2015 as well (corresponding red curves in Figure 4e). A positive anomaly in SR intensity in the H_{EW} field component at the BOU station was observed near 21 UT in the transition month of February, 2015 (corresponding red curve in Figure 4e). This anomaly could be attributed to the increased lightning activity nearby in the coastal region of Mexico.

3.2. Results Based on Independent Lightning Observations

The SR are inherently a long-wavelength phenomenon and in single-station observations cannot resolve the subcontinental distribution of lightning sources. In order to further strengthen our SR-based results and to reveal the specific geographical regions from which the intensification of SR predominantly originate we analyze lightning distributions provided by independent observational methods (satellite-based optical and ground-based VLF) in selected months when the strongest intensification in SR is documented: April 1997 (Figure 5) for the 1997/98 event as well as December 2014 (Figure 6) and February 2015 (Figure 7) for the 2014/15 super El Niño event. As references we use the lightning distributions from the same months but one year earlier: April 1996 (under La Niña condition) as well as December 2013 and February 2014 (under non-ENSO condition), respectively. We carry out this kind of analysis only for the Asian chimney region where the UT time distributions of normalized SR intensity shown in Figures 2–4 provide evidence for the most probable locations of important changes in lightning activity.

High-flash-rate lightning activity was observed in Southeast Asia and the MC in the ENSO transition month of April 1997, with increased lightning activity also detected in northeast India and the Himalaya region (where instability analysis was accordingly undertaken, Section 3.3) as observed by the OTD satellite (Figure 5). The overall lightning increase for the MC in Figure 5 between April 1996 and April 1997 amounted to ~35%. This behavior is consistent with the enhanced SR intensity documented in Figures 2f and 2g in the same transition month, but with different percentage increments (~350% in E_Z at NCK and ~20% in H_{EW} in RID). The large percentage departures relate to the different methods for the lightning observations. In general, OTD underestimates the lightning activity in unsampled active regions over the monthly time scale but can identify weak flash characteristics (event/flash, group/flash, radiance/flash, duration/flash) in India (Beirle et al., 2014). The mean radiance per flash in India is only half of the global mean and higher values

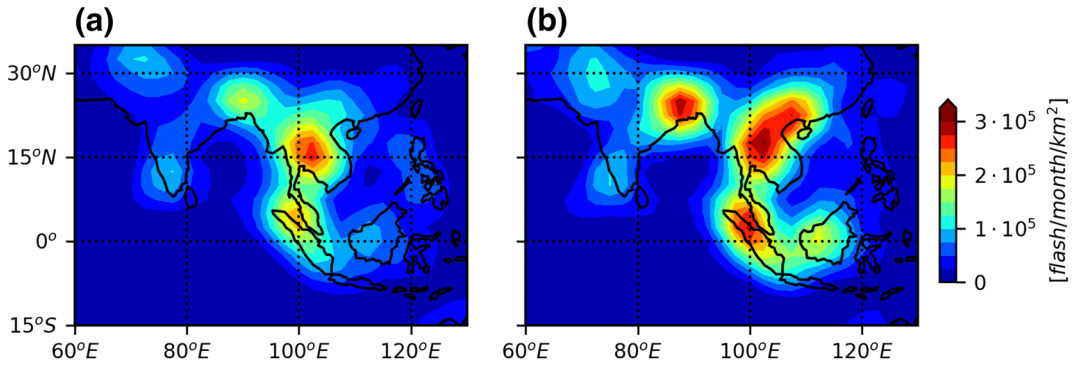

Figure 5. Flash number density for the Maritime Continent (MC) and India observed by the Optical Transient Detector satellite in (a) April 1996 and (b) April 1997. A ~35% increase in flashes was observed between April 1996 and April 1997.

observed over Indonesia (Beirle et al., 2014). Therefore, it is possible that the lightning activity can appear with different importance in the SR measurements based on extremely low frequency (ELF, 3 Hz–3 kHz) electromagnetic radiation of lightning and on the optical observation by the OTD satellite. The OTD activity was sustained for most of 1997 to the peak in the warm phase in November 1997 (but not shown here), while the SR-measured lightning diminished markedly after April 1997. This apparent discrepancy between two independent measures of lightning activity is not presently understood.

Given the evidence in multistation SR measurements shown in Figures 3 and 4 for greater regionally resolved lightning activity in the ENSO transition months, and in recognition of the importance of oceanic lightning in this MC chimney, interest arose in the comparison with continuously available surface lightning network data. Observations from the WWLLN have been examined for two transition months (December 2014 and February 2015) over a wide area (90°E to 160°E and 35°S to 15°N) of the MC in Figures 6 and 7, respectively. In both figures, comparison maps are made for the same months in two separate years, and for both daytime (10:00 a.m.–10:00 p.m., centered at 4:00 p.m.) and nighttime (10:00 p.m.–10:00 a.m., centered at 4:00 a.m.) conditions. Also included in each plot (Figures 6e and 7e) are the local diurnal variations of the WWLLN-observed lightning strokes averaged over each month. Especially noteworthy in Figure 6 is the marked increase in lightning activity over northern Australia and an average increase of ~25% strokes from December 2013 to December 2014. Also noteworthy in Figure 7 is the pronounced increase in activity over northwest Australia and the prevalent areas of activity immediately adjacent to land-ocean boundaries (Sumatra, Borneo, NW Australia, Gulf of Carpentaria (Australia)). The average increase in strokes in the transition month February 2015 is ~15%. The full diurnal comparisons in both Figures 6 and 7 show more lightning in the ENSO transition month in nearly every local hour.

In conclusion, based on independent lightning observations (OTD and WWLLN), lightning activity was more intense in the Asian/MC chimney region in the transition months of the two super El Niño events than in the same months of the preceding years under La Niña or non-ENSO conditions. These independent lightning observations are consistent with inferences based on SR observations with inherently coarser spatial resolution.

3.3. Results Based on Analysis of CAPE

CAPE is known from previous studies to be a robust indicator of lightning activity (Pawar et al., 2011; Williams & Stanfill, 2002; Williams et al., 2002). Given the marked enhancement in lightning activity documented in the SR observations in the ENSO transition month of April 1997, and the suggestion in the diurnal variation that the primary source region was the Indo-Gangetic Plain south of the Himalaya, a collection of thermodynamic soundings from this region was evaluated for CAPE, and compared with like soundings in April 1996 as a nontransition month and with April 1998 as a declining warm phase

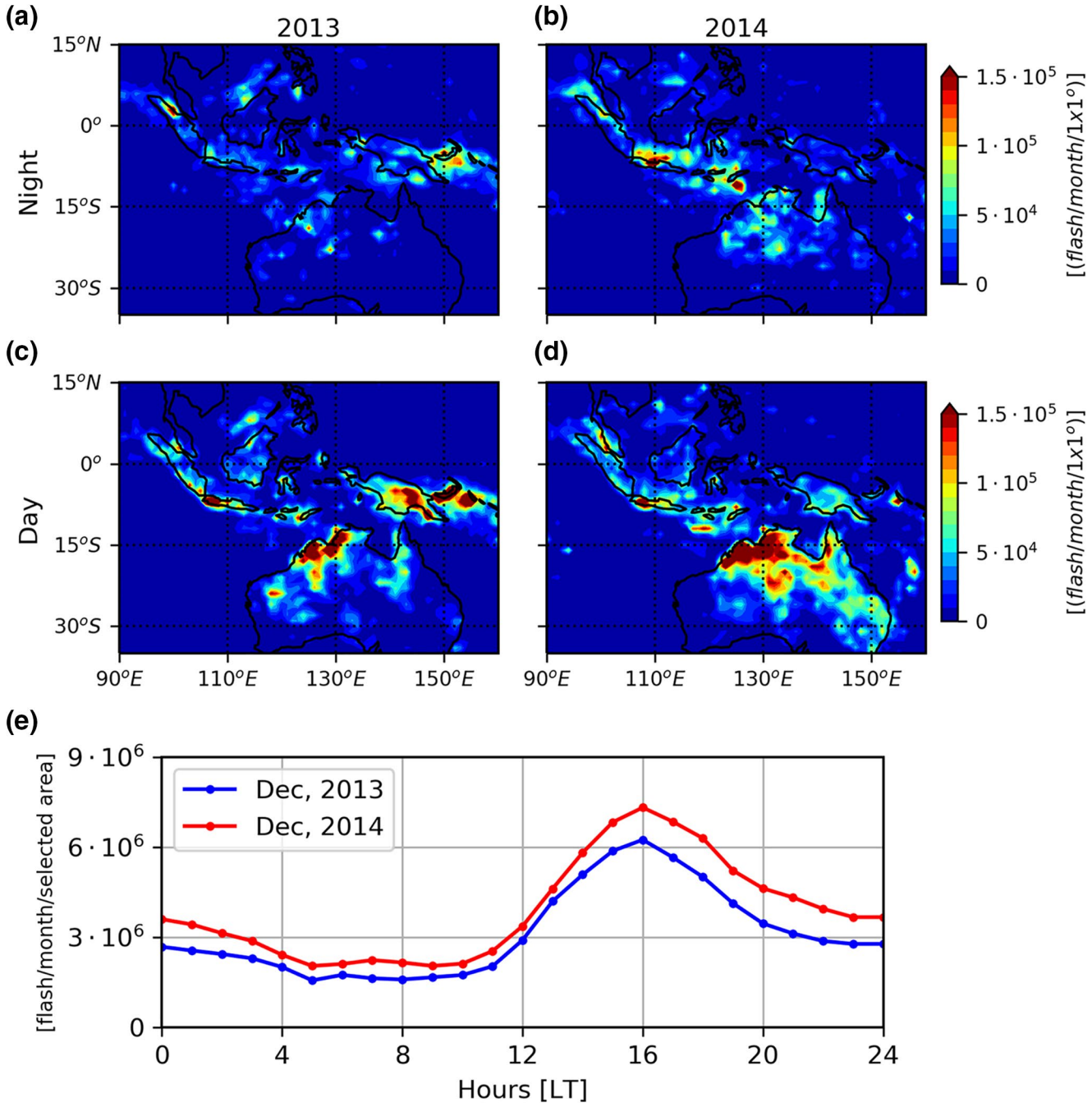

Figure 6. Flash rate observed by the World Wide Lightning Location Network (WWLLN) network in (a) December 2013 between 22 and 10 LT ("nighttime"), (b) December 2014 between 22 and 10 LT ("nighttime"), (c) December 2013 between 10 and 22 LT ("daytime"), and (d) December 2014 between 10 and 22 LT ("daytime") for the MC as well as northern Australia. (e) Diurnal variation in local time for the entire month of December, both during the cold phase (December 2013, blue) and during the transition to warm phase (December 2014, red). The conspicuous increase in lightning activity in Australia is consistent with the SR diurnal enhancements noted in the same month in Figures 3 and 4, and with the convective available potential energy (CAPE) comparisons appearing in Figure 10.

month. The comparisons are shown in Figure 8 for a representative selection of radio-soundings available within the region of interest for all three April periods. All available soundings within each month for each station selected were included in the monthly averages. Substantial increases in CAPE are noted in the Indo-Gangetic Plain where lightning enhancements were also documented in Figure 5. The six stations

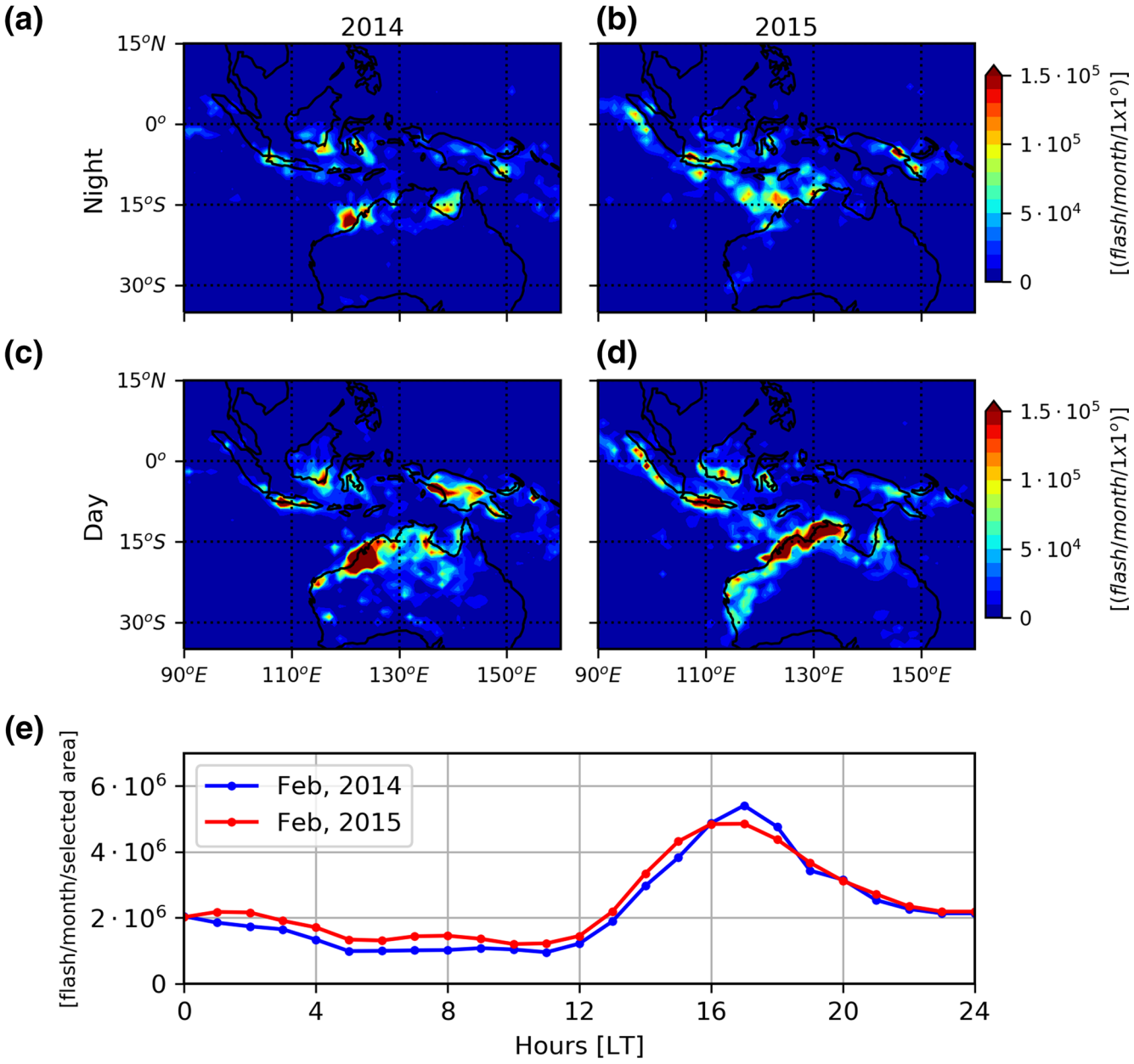

Figure 7. Flash rate observed by the WWLLN network in (a) February 2014 between 22 and 10 LT ("nighttime"), (b) February 2015 between 22 and 10 LT ("nighttime"), (c) February 2014 between 10 and 22 LT ("daytime"), and (d) February 2015 between 10 and 22 LT ("daytime") for the MC and including northern Australia. (e) Diurnal variation in local time for the entire month of February, both during the cold phase (February 2014, blue) and during the transition to warm phase (February 2015, red). Nighttime activity immediately adjacent to land regions is evident in many cases. The conspicuous increase in lightning activity in Australia in all but three LT hours is consistent with the SR diurnal enhancements noted in the same month in Figures 3 and 4, and with the CAPE comparisons appearing in Figure 10.

selected in Figure 8 were located in the inferred lightning-active region of India where CAPE increases were also documented. It can be seen that in the majority of cases, both the 0Z and the 12Z soundings show substantially greater CAPE in the transition month of April 1997 than in the cold phase of April 1996, sometimes by a factor-of-two, qualitatively consistent with the lightning contrast. Regarding the comparison between the transition phase and the warm phase, Figure 8 shows a mix of stations showing maximum instability in the transition phase (dominant behavior) and other stations showing greater instability in the declining warm phase. This mixed behavior is not at variance with the SR-based lightning

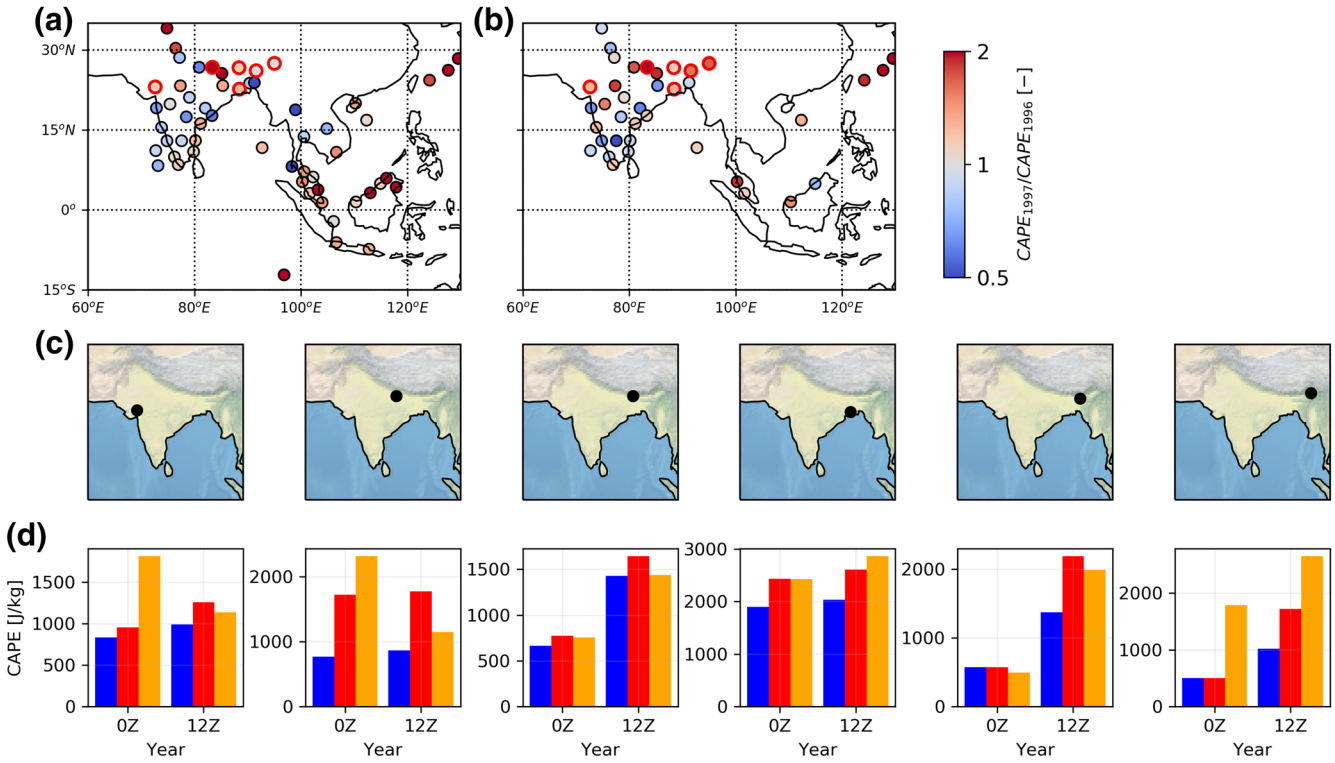

Figure 8. CAPE documentation based on radio-soundings between April 1996, April 1997, and April 1998. (a–b) Ratio of monthly average CAPE values ($CAPE_{April,\ 1997}/CAPE_{April,\ 1996}$) at different radiosonde stations in the MC and India (a) at 0Z and (b) at 12Z. (c) Location of six selected radiosonde stations in the Indo-Gangetic Plain and (d) monthly average CAPE values for these six stations. Blue, red, and orange bars correspond to April 1996 (cold), April 1997 (transition), and April 1998 (declining warm), respectively.

observations showing evidence for intensification in both the transition and the warm phase of this super El Niño event.

CAPE is the positive area on a tephigram bounded by the environmental temperature sounding on the left and by the moist adiabat on the right. The difference between these two boundaries is the parcel buoyancy and usually amounts to 10°C or less, making CAPE a delicate quantity. To ascertain whether the CAPE increases documented in Figure 8 from the cold to the transition phase in India are attributable either to a systematic reduction in the environmental temperature or to an increase in the moist adiabat, a special differential analysis was undertaken. Based on the evidence in an earlier study (Williams & Renno, 1993) for a zero-CAPE intercept of 23°C in the wet bulb adiabat temperature for a large number of tropical soundings, all environmental temperatures aloft within the troposphere were compared with the parcel temperature associated with that special moist adiabat, for both April 1996 and April 1997. In the same manner, all the parcel temperatures on the moist adiabat in every sounding were compared with the parcel temperatures associated with that special moist adiabat and within the troposphere, for both April 1996 and April 1997. The results of this analysis for three sample stations all showing increased CAPE from April 1996 to 1997 are shown in Figure 9. These findings support the idea that a somewhat colder middle-troposphere environment in April 1997 is the main cause for the CAPE increase, and that no obvious systematic change is apparent in the moist adiabat.

For the instability analysis for the second super El Niño event (2014/15), it is noted that the ENSO transition months (red arrows in Figures 3b and 4b) lie in NH winter, and so the domain of interest shifts into the Southern Hemisphere, relative to that shown in Figures 8 and 9. The contribution of the active lightning in NW Australia has already been documented in Figures 6 and 7 for this time period. For CAPE analysis shown in Figure 10, all three ENSO phases (cold in blue, transition in red, and warm in orange) have been examined. Consistent with the lightning behavior, the greatest CAPE values are found in the transition period at nearly all stations in Australia available for the analysis.

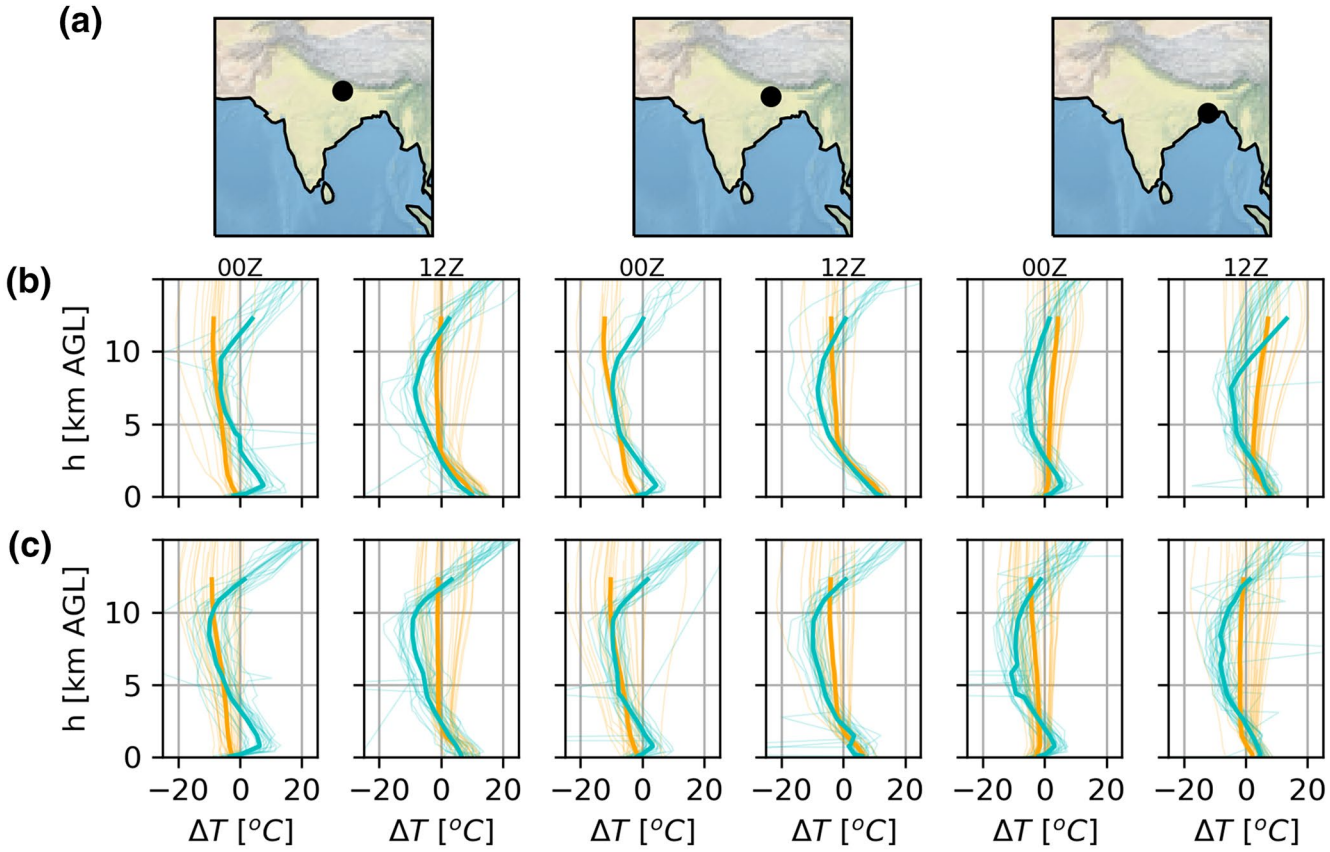

Figure 9. Diagnosis of two contributions to CAPE increases from April 1996 to April 1997. The two contributions are the environmental temperature (Tenv–Tref) (turquoise colors) and the surface moist adiabat (Tpar–Tref) (orange colors). Thick curves are averages of all soundings in the respective month. (a) Selected locations of sounding sites in India, (b) comparisons in turquoise and orange for all soundings in April 1996, and (c) comparisons in turquoise and orange for all soundings in April 1997.

4. Discussion

The mainstay of this work is represented by the multistation Schumann resonance measurements, but the ramifications of the work extend much further to tropical convective adjustment to temperature change, to the response of lightning to ENSO thermodynamic forcing, and to the monitoring and prediction of global climate change. Accordingly, a number of topics are worthy of separate discussion below.

4.1. Ramifications of UT Diurnal Variations of Schumann Resonance Intensity for Dominant Chimney Response

The UT time distribution of the observed anomalies in SR intensity preceding the two super El Niño events show different characteristics. For the transition months of the 1997/98 super El Niño event the anomalies appear predominantly near 10–12 UT which is the characteristic activation time of the western part of the Asian chimney including the Indian subcontinent and Pakistan (Albrecht, 2016; Blakeslee et al., 2014). On the other hand, the SR intensity increases throughout the whole 0–24 UT time period in connection with the super El Niño event of 2015/16, which hints at a global response i.e., all chimneys involved) in lightning activity. However, in this event the greatest increase of SR intensity often appears in the 6–12 UT period which again can be attributed to increased lightning activity in the specific regions of the Asian/MC chimney. In this respect the two super El Niño events are similar.

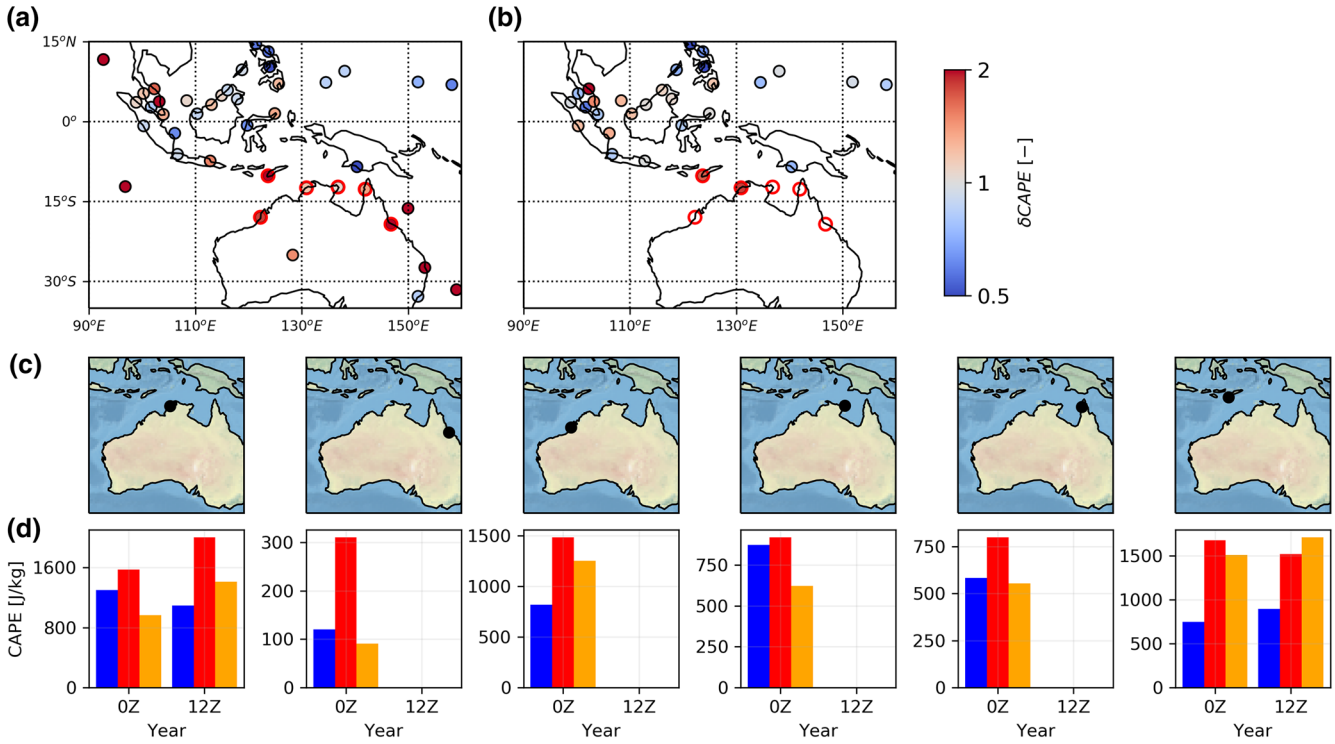

Figure 10. CAPE documentation between December 2013, December 2014, and December 2015. (a–b) Ratio of monthly average CAPE values ($CAPE_{December, 2014}/CAPE_{December, 2013}$) at different radiosonde stations in the MC as well as northern Australia (a) at 0Z and (b) at 12Z. (c) Location of six selected radiosonde stations in northern Australia and (d) monthly average CAPE values for these stations and for both 0Z and 12Z soundings. Blue, red, and orange bars correspond to December 2013 (cold), December 2014 (transition), and December 2015 (warm), respectively.

4.2. The Contrast in Onset Behaviors for the Two Events

The known difference in the onset behaviors of the two super El Niño events (Lim et al., 2017) also appear in the SR intensity variations. The earlier event showed a simpler evolution. The anomalous increase of SR intensity is confined to a 2–3 month interval preceding the super El Niño event of 1997/98. This period of February to April coincides with the premonsoon time in India. On the other hand, the 2015/16 super El Niño occurred in two steps which is in line with our SR observations. The anomalous increase of SR intensity was first observed in September 2014 exactly when the ENS-ONI index turned from near zero to a markedly positive value. But then, in the subsequent months, the warm phase appeared to be aborting. The reignition of the 2015/16 super El Niño occurred in February 2015 and amplified this warm episode into a super El Niño by the end of 2015 (L. Chen et al., 2017; Dong & McPhaden, 2018). In this respect, this event behaved like many others in maximizing near the end of the calendar year (see Table 1 and discussion in Section 4.6). The anomalies in SR intensity already appeared in December 2014 and reached their maximum in February 2015. These observations strongly suggest that the SR intensity provides early evidence for the occurrence of the warm ENSO periods at least in the case of the strongest "super" El Niño-like events.

4.3. Comparisons with Previous Lightning Analyses on the ENSO Time Scale

Many published studies address the ENSO-lightning relationship, and in most of them the warm and cold phases are the exclusive scientific focus, not the transition periods. Some of these earlier studies refer simply to El Niño "years" and La Niña "years" (M. N. Kulkarni & Siingh, 2014; M. K. Kulkarni et al., 2015; Kumar & Kamra, 2012; Tinmaker et al., 2017) while others select specific monthly sequences as "El Niño" and "La Niña" episodes, based on various ENSO temperature indices (Chronis et al., 2008; Hamid et al., 2001; Satori et al., 2009; Siingh et al., 2017; Wu et al., 2012, 2017; Yoshida et al., 2007). But in either procedure

the transition period from cold to warm phase, frequently amounting to several months, is either left out of the analysis, or a portion is included with the warm phase. One important exception is the study by Guha et al. (2017) in which emphasis is given to the warm-to-cold transition in the 2009/2010 ENSO event that can be seen in Figure 1. Even in earlier studies making use of the pressure-based Southern Oscillation Index that considered only temperature and rainfall variations (e.g., Halpert & Ropelewski, 1992) over tropical continental regions, primary attention was given only to the "high" and "low" phases of ENSO, and not their transitions.

This documented focus in previous ENSO/lightning studies is understandable given the general interest in the response of lightning activity to surface air temperature (e.g., Williams et al., 2019). The El Niño periods exhibit the warmest SST anomalies and the La Niña periods the coolest ones. But the ENSO indices are continuously variable measures of SST imposed by the ocean, and the conspicuous lightning enhancements in the transition period points to thermodynamic/convective disequilibrium, as elaborated on in Section 4.4. Both the land surfaces and the atmospheric column are adjusting to the change forced by the increase in the temperature of the ocean that surrounds the land masses of the MC during the transition period. Both these adjustments can contribute to increased updraft strength in the deep moist convection that accounts for the lightning activity.

4.4. ENSO Context for Key Thermodynamic Changes

The changes in key thermodynamic quantities CAPE and cloud base height are possible contributors to the regional lightning enhancements in the two super El Niño events. But the physical basis for the thermodynamic changes deserves explanation in the context of the evolving ENSO event. Fortunately, this explanation is buttressed by the evidence that these two events show generally the same consistent seasonal evolution as many other super El Niños (Allen et al., 1996), as discussed also in Section 4.6. Given that the lightning activity in the MC is invigorated in both events, we will focus in this discussion on the telecommunicated response of that chimney to oceanic convection further east.

In the early part of the calendar year, the ocean is already delivering anomalously warm surface water to the central and eastern equatorial Pacific Ocean. The MC to the west remains in cold La Niña condition at this time. Both anomalous sensible and latent heat are transferred to the atmosphere over the warm equatorial anomaly. Deep moist convection consequently begins to develop there, warming the local atmosphere further by the latent heat of condensation and freezing, which in turn causes an expansion of the atmosphere and the creation of an anomalous low pressure zone that enhances the low level convergence. This upwelling in the central Pacific subjects the cold MC to the west to anomalous subsidence. The effect of this subsidence is two-fold: (1) atmospheric condensate there begins to evaporate/sublimate with consequent anomalous cooling of the local troposphere and increase in CAPE and (2) the reduction in atmospheric opacity to incoming sunlight.

The increased shortwave radiation promptly warms the underlying land surface of the MC. The high-heat-capacity ocean there is also warmed, and the SST there is generally increasing steadily throughout the calendar year (Allen et al., 1996). The anomalous subsidence in the MC and the local tropospheric cooling due to evaporation/sublimation of condensate leads to a developing positive anomaly in the mean sea level pressure beneath this chimney. This telecommunication has been amply documented in satellite observations of earlier ENSO events (Klein et al., 1999) showing maximum reductions in cloud cover during the transition period and the warm phase. The telecommunication is also widely recognized as the basis for enhancements in surface air temperature and for reductions in rainfall over land in all three chimney regions (Allen et al., 1996; Halpert & Ropelewski, 1992; Trenberth et al., 2002). This large-scale reduction in tropical rainfall is also manifest in hydrological records for large drainage basins (Amerasekera et al., 1997). The widespread rainfall reduction is also deemed responsible for the reduction in surface dew point temperature over land areas, on account of reductions in soil moisture. This reduction together with the higher surface temperature both contribute to an increased dew point depression and a raising of the cloud base height over land in the warm phase. Increasing lightning activity with increasing cloud base height has been shown earlier by Williams et al. (2005).

The findings described in Section 3.3 (Figures 8–10) suggest that increases in CAPE during a process of convective adjustment from cold phase to warm phase is the most important thermodynamic factor in accounting for the documented lightning increases in Figures 2–7. Considerations for the response of lightning flash rate to CAPE are found in Williams and Stanfill (2002). Updraft speed varies as the square root of CAPE, but if the lightning rate of a thunderstorm varies as the fourth power of the updraft speed (Boccippio, 2001), then a doubling of CAPE amounts to a four-fold increase in lightning rate. Occasional factor-of-two increases in CAPE have been shown in Figures 8 and 10.

Checks for possible increases in cloud base height in the transition months as a possible contributor to the lightning increases were unsuccessful, but some indications of increasing cloud base height in the warm phase over land were identified (but not shown here). This effect may contribute to the enhanced lightning that was noted during the warm phase of both super El Niño events considered here.

This study sheds some new light on the subtle issue of convective adjustment in the tropical atmosphere and the time scale needed for that to occur. The smallness of CAPE is some measure of convective adjustment, and in early modeling work a moist neutral configuration was often assumed. Lightning activity is perhaps the most sensitive indicator known for the departure from convective equilibrium. The shortcoming of using lightning flash rate alone as an indicator over an area is the ambiguity between flash rate per convective cell versus number of cells per unit area (Williams et al., 2000). It is widely recognized that the diurnal time scale is not sufficient for convective adjustment and a large flash rate is often evident after CAPE attains its maximum value, especially over land (Williams, 2020; Williams et al., 2000). On the longer semiannual time scale (Williams, 1994), one finds a conspicuous lightning response to surface air temperature (Williams, 2020), suggesting an insufficient time for convective adjustment. The solution to the issue of the flash rate per convective cell versus areal concentration of cells has not yet been established. On the annual time scale, the evidence from the satellite optical record (Williams et al., 2000) is that there is rather little change in the mean flash rate per cell but a considerable change in the number of cells per unit area.

The time scales involved with the enhanced CAPE in the super El Niño events are comparable to semiannual time scales, and so the evidence for CAPE accumulations over large areas is quite plausible from this additional perspective.

While CAPE remains the main metric for departures in convective adjustment, the other key thermodynamic consideration is water vapor and the Clausius-Clapeyron relation, with its fundamental temperature sensitivity ~7% per °C (Williams, 2020). As one transitions from the cold to the warm phase in ENSO, the maximum possible water vapor mixing ratio, latent heat of condensation, wet bulb potential temperature, and moist static energy all increase. This may have some bearing on the secondary maximum in lightning activity in the peak warm phase, even when CAPE shows indications of a decreasing trend (Figures 8 and 10).

The demonstrated response of CAPE over land to the transition from cold phase to warm phase on the interannual time scale has obvious connections to claims that CAPE should increase in a warmer climate on still longer time scales (Agard & Emanuel, 2017; J. Chen et al., 2020; Romps, 2016; Romps et al., 2014; Saha et al., 2017; Williams, 2012). The role of the Clausius-Clapeyron relation has also been invoked here. The anticipated increases in continental tropical cloud base height in the warm phase of ENSO, with contributions (as a dew point depression) from both elevated surface temperature (Allen et al., 1996; Halpert & Ropelewski, 1992) and decreased dew point temperature (Trenberth et al., 2002), is also deserving of further analysis, especially given the evidence for an effect on lightning activity.

4.5. Possible Aerosol Effects on Lightning Activity

The role of aerosol in the form of cloud condensation nuclei in increasing lightning activity is increasingly recognized (Fan et al., 2018; Hu et al., 2019; Stolz et al., 2017; Thornton et al., 2017; Q. Wang et al., 2018b; Williams, 2019). Though studies of changes in cloud condensation nuclei (CCN) have not been undertaken over ENSO cycles, it can be expected that CCN concentrations will increase during the subsidence phase over land areas during the warm phase. The observations presented here showing a maximum in lightning

activity in the transition to the warm phase, with distinct reductions in lightning activity in the subsequent warm phase, suggest that thermodynamics (e.g., CAPE) is playing the leading role in modulating the lightning. It should be noted however that a workable satellite method (Rosenfeld et al., 2016) is now available for documenting CCN on chimney scales (M. Wang et al., 2018a), and that such methods could now be deployed to investigate the matter further. This task is however beyond the scope of the present study.

4.6. Historical Context for the Two Super El Niño Events

The two most recent super El Niño events in the climate record have been selected for analysis here because of the availability of coincident lightning/Schumann resonance observations. As shown in Figure 1, these two events stand out clearly with peak ONI indices exceeding 2.0°C and both with dominant influences on the global temperature record. A search of the complete ONI index history back to 1871 shows only four other extreme events (December 1877; November 1888; December 1972; January 1983) for the 150-year history of SST measurements, and so a total of six events. They are summarized in Table 1. The 1972 event formed the basis for an early SR investigation of ENSO (Williams, 1992). Given the evidence for globally extensive SST anomalies (Allen et al., 1996) and back-to-back La Niña/El Niño events in that time period, perhaps the global correlation in that study is more plausible. The 1983 event, showing the more traditional positive SST anomaly only in the eastern Pacific Ocean (Allen et al., 1996) formed the basis for a textbook on ENSO (Philander, 1990).

It is often stated that no two ENSO events are alike. One can study this claim further by examining the global thermodynamic context of the six super El Niño events, two of which have been shown to exhibit lightning enhancements during the transition phase in the present study. For thermodynamic context, we appeal to the global anomaly maps of SST (e.g., Allen et al., 1996; https://climate.nasa.gov/climate_resources/185/sea-surface-temperature-anomaly-timeline-1982-2017/) available over the same time period. The two very strongest events with highest ENS-ONI indices are December 1877 (+2.665°C) and November 2015 (+2.653°C). These two events also stand out as exhibiting positive SST anomalies that are zonally continuous and so surround the three tropical continental lightning chimneys. This behavior may help guarantee that continental regions are subjected to large scale subsidence that will serve to enhance their "continental response." It may also serve to suppress the continental monsoonal circulation that is a major source of widespread continental rainfall during the La Niña phase (Allen et al., 1996). These two super El Niños are also both preceded by La Niña events with negative SST anomaly pervading the entire tropical belt. These consistent features help explain a robust global increase in lightning activity during the transition period, and also the observations that all three chimney regions are involved in the lightning enhancement (at least for the 2014/15 event), as discussed previously in Section 4.1.

Consideration of SR/lightning behavior has also been given to notably weaker ENSO events with ONI index in the range between 1.0°C and 2.0°C, four of which can be seen in the short record of Figure 1. Twenty-five such events are evident in the longer ONI record from 1870 to 1995. The thermodynamic documentation (Allen et al., 1996) of most of these events do not show a global increase in SST anomaly throughout the tropical domain, and less than half of them show well-defined cold oceanic regions pervading and surrounding the MC in advance of the warm phase. These differences with the collection of six super El Niño cases may provide partial explanations for why the lightning response to the weaker events does not show the same consistent behavior chimney-by-chimney that we have shown for the exceptional 2015 event (Table 1).

Table 1
Summary of the Six Top Super El Niño Events in 150 Year Period: 1870–2020

ENSO year	Month	ENS-ONI index (°C)	Character of global + SST anomaly
1877	December	+2.665	Zonally complete
1888	November	+2.226	Incomplete
1972	December	+2.078	Incomplete
1983	January	+2.513	Incomplete
1997	November	+2.555	Incomplete
2015	November	+2.653	Zonally complete

One other consistent feature of Table 1 is the well-recognized tendency for El Niño events to predominate in NH winter (November, December, January). In line with the notion so important for the present study, that El Niño involves ascent over oceans and subsidence over land, this seasonal behavior may be attributable to solar heating of the more expansive Southern Hemisphere ocean and favored subsidence over the cold North

American continent from the upwelling in the central and eastern equatorial Pacific Ocean (N. Renno, personal communication, 2020).

4.7. Connection with the Recent Hiatus in Global Warming

The two super El Niño events selected for analysis in this study are also interesting because they set boundaries on the period referred to as the "hiatus in global warming," generally taken to be the interval 1998–2014. This hiatus period can be visually identified in the NASA GISS record of global surface air temperature anomaly in Figure 1. Several global temperature records have been shown to be statistically flat in this time frame (Williams et al., 2019), whereas the periods before and after show substantial warming trend. The record of global lightning activity from the NASA LIS in space is also statistically flat in this special time interval (Williams et al., 2019).

The physical origin of the hiatus in global warming is not well known, though it is generally believed that it represents a period of enhanced heat uptake by the oceans, in marked contrast to the bounding ENSO periods characterized by the giving up of ocean heat. It is valuable to contrast the rates of warming dT/dt in the super El Niño events with an upper bound on the rate of warming during the much longer hiatus period. Based again on Figure 1, the tropical warming rate is of the order of 2°C per year, and the global warming rate is of the order of 0.5°C per year. In contrast, a reasonable (visual) bound on the rate of global warming over the nominal decade of the hiatus is 0.1°C per 10 years = 0.01°C/yr. Given the 50–200-fold difference in these estimates, it is not surprising that one has a clear lightning signature in one circumstance and not in the other.

The strong tendency for maxima in global lightning activity in the ENSO transitional periods adjacent to the hiatus period is evidence for greatest global departure in convective equilibrium in the transition periods. The evidence for secondary lightning maxima in the peaks of the warm phase is also noted.

4.8. Connection Between Schumann Resonance Intensity and Lightning Flash Rate

A long-standing assumption in interpretations of Schumann resonance background signals from relatively compact chimney sources is that the measured intensity is proportional to the lightning flash rate (Boldi et al., 2018; Clayton & Polk, 1977; Dyrda et al., 2014; Heckman et al., 1998). The SR/OTD and SR/WWLLN comparisons documented in Section 3.2 suggest that this assumption may not always be valid. Implicit in the linear relationship between SR intensity and flash rate is the invariance of the mean charge moment change (CMC) per flash but, in reality, this quantity could vary with meteorological scenario, including the phase of ENSO. The WWLLN is recording only high-energy ground flashes, and this may provide some explanation for why the interannual changes in WWLLN stroke rates (∼20%) are smaller than changes documented with SR and optical methods. Further comparisons between Schumann resonance intensity and flash rates measured by more conventional detection methods (optical and radio frequency) are needed to sort this out. Comparisons of this kind during the declining warm phase of the super El Niño events are particularly needed. The Global Lightning Mappers on GOES-16 and GOES-17 satellites will be particularly valuable in this regard as they provide the same continuous observations of specific regions that are also available with SR observations.

4.9. Advantages of SR as a Monitor for Global Lightning

One of the main advantages of the SR-based monitoring of global lightning activity is that it does not suffer from the detection efficiency problems which are inherent with other lightning detection methods (Boccippio et al., 2000; Hutchins et al., 2012; Said et al., 2010). Lightning radiated waves in the SR band (<100 Hz) have extremely weak attenuation (<0.5 dB/Mm; Wait, 1970) and all lightning strokes with vertical extent contribute to the measured electromagnetic fields. However, to reveal the best possible CMC-based spatial distribution of global lightning corresponding to the months with increased SR intensity, a geophysical inversion algorithm ingesting multi-ELF-station spectral information is required (Nelson, 1967; Nickolaenko

& Hayakawa, 2014). Our group is working on the implementation of such an algorithm (Bozóki et al., 2019; Prácser et al., 2019) which will hopefully contribute to the better understanding of variations in lightning activity on the ENSO timescale. Time series data from a large number of ELF receivers worldwide have been assembled for the period of the second super El Niño and inversion calculations are planned as a future effort.

4.10. Superlative Lightning Response of the MC to ENSO Forcing

The history of ENSO-lightning studies has shown clearly that the MC stands out among the three continental "chimneys" in its lightning response to ENSO forcing. The strongest evidence here is found in a global study by Sátori et al. (2009) but a larger volume of secondary evidence lies in the great majority of ENSO-lightning investigations centered on SE Asia/India/Indonesia, all component regions of the MC in having a mix of land and ocean within the tropical belt (Ahmad & Ghosh, 2017; Hamid et al., 2001; Kumar & Kamra, 2012; Tinmaker et al., 2017; Yoshida et al., 2007; Yuan et al., 2016). This focus on the MC is also consistent with the finding in Section 4.1 that the MC dominated the three tropical chimneys in the response to ENSO forcing.

Previously suggested explanations for the MC's superlative lightning response have centered on a common theme in the present study: thermodynamic disequilibrium. Considerable time is needed for land areas adjacent to oceans to adjust to a warmed ocean. The contrasts in temperature between land and ocean drive land-sea breeze circulations (Chronis et al., 2008; Hamid et al., 2001; Williams & Mareev, 2014; Yoshida et al., 2007) which in turn affect the updraft speeds that are so important for lightning activity. The superlative length of the land-ocean boundary in the MC in comparison with the other continental chimneys is readily apparent.

Considerations of the local diurnal variation of lightning on a global basis (Blakeslee et al., 2014; Figure 4; Cecil et al., 2015) have shown that while the typical 4:00 p.m. maximum in lightning activity prevails over large portions of the American and African continents, the situation with the MC is considerably more complicated. For example, the complications of the Indo-Gangetic Plain in proximity to the Himalayan Range in India have previously been addressed in interpreting the SR intensity variations in Universal Time (Figures 3 and 4). Given the limitations of Schumann resonance observations in spatial resolution for the lightning source, use has been made of the WWLLN VLF network observations to study the local diurnal variation of lightning over the MC in two important transition months: Decembers of 2013 and 2014 (Figure 6) and Februaries of 2014 and 2015 (see Figure 7). For this analysis the 24-h day has been divided in half, with one 12-h period (10–22 LT) centered on the 4:00 p.m. local maximum and selected as a "daytime" interval and the other 12-h period (22–10 LT) centered on 4:00 a.m. local time to define "nighttime" conditions. The lightning activity in these NH winter months is dominated by activity along the NW coast of Australia. The nighttime activity is frequently associated with coastlines, as for example, along the SW coast of the island of Sumatra in Figure 7. In the analyses of the full diurnal variation of the lightning in both Figures 6 and 7, the appreciable nighttime contribution is evident and amounts to about half of the daytime contribution.

A similar comparison can be found in the earlier ENSO/lightning study over Indonesia by Hamid et al. (2001) using LIS observations of lightning from space. This two-to-one daytime/nighttime contrast can be compared with daytime-dominant lightning behavior at land stations removed from the MC (see sample diurnal variations in Williams and Heckman (1993) in which the daytime/nighttime lightning ratio lies in the range of 5–20). The nighttime lightning in the MC is relatively more frequent than in the other two chimneys, and that is, an important component of the ENSO lightning response, even though the total lightning activity within the MC often trails that in the other two chimneys, climatologically speaking.

5. Conclusions

In the present study we aimed to identify common signatures in the temporal evolution of two "super" El Niño events in 1997/98 and 2015/16 by investigating Schumann resonance intensity. The analyses directed our attention to the transition months preceding these events when ENSO turned from the cold La Niña

to its warm El Niño phase. Intensification of SR occurred in the transition months preceding both super El Niño episodes, supporting a key role for thermodynamic disequilibrium and suggesting that SR intensity may play a precursory role for the occurrence and magnitude of these extreme climate events. In addition, SR intensity records mirrored also some of the important differences between the onset mechanisms of the two events. Our results suggest that the observed SR intensifications corresponding to the 1996/97 super El Niño event originate from Southeast Asia, the MC, and India while a global response of lightning activity is indicated for the 2015/16 super El Niño event. Indeed, the intensification of lightning activity has been confirmed in selected months by independent lightning observations as well. The peak El Niño times lead the maxima in global temperature by times of order 2–3 months, and consequently the major upsurge in lightning activity within the MC in the super El Niño events (preceding by ∼6 months the times of maximum ENS-ONI index) serves as predictions of peak global warming with lead times ∼9 months.

Data Availability Statement

The v0.1 gridded satellite lightning data set was produced by the NASA LIS/OTD Science Team (Principal Investigator, Dr. Hugh J. Christian, NASA/Marshall Space Flight Center) and is available from the Global Hydrology Resource Center (https://ghrc.nsstc.nasa.gov/home/). The authors wish to thank the World Wide Lightning Location Network (http://wwlln.net), a collaboration among over 50 universities and institutions, for providing the lightning location data used in this study. Radio-sounding data are available from the webpage of University of Wyoming (http://weather.uwyo.edu/upperair/sounding.html). The SR data used to produce results are available at https://zenodo.org/record/4276361#.X7Lrx82nfCI. Special thanks are due to Dr. Larry Oolman at the University of Wyoming for generous provision of additional thermodynamic quantities from radio-soundings. Discussions with N. Renno on multiple aspects are appreciated. The authors highly appreciate the helpful and constructive criticism of Richard Blakeslee and two anonymous reviewers.

Acknowledgments
The work of T. Bozóki and G. Sátori was supported by the COST Action CA15211 and by the National Research, Development, and Innovation Office, Hungary-NKFIH, K115836. The contributions of Earle Williams, Anirban Guha, and Yakun Liu for this work have been supported by the Grainger Foundation and by the US National Science Foundation (Grant # 6942679).

References

Agard, V., & Emanuel, K. (2017). Clausius-Clapeyron scaling of peak CAPE in continental convective storm environments. *Journal of the Atmospheric Sciences*, *74*(9), 3043–3054. https://doi.org/10.1175/JAS-D-16-0352.1

Ahmad, A., & Ghosh, M. (2017). Variability of lightning activity over India on ENSO time scales. *Advances in Space Research*, *60*(11), 2379–2388. https://doi.org/10.1016/j.asr.2017.09.018

Aich, V., Holzworth, R., Goodman, G., Price, C., & Williams, E. (2018). Lightning: A New Essential Climate Variable. *EOS*. *99*, https://eos.org/science-updates/lightning-a-new-essential-climate-variable

Albrecht, R. I. (2016). Where are the lightning hot spots on Earth? *Bulletin of the American Meteorological Society*, *97*(11), 2051–2068. https://doi.org/10.1175/BAMS-D-14-00193.1

Allen, R., Lindesay, J., & Parker, D. (1996). *El Nino Southern Oscillation and Climatic Variability*, Clayton, Australia: CSIRO Publishing.

Amerasekera, K. N., Lee, R. F., Williams, E. R., & Eltahir, E. A. B. (1997). ENSO and the natural variability in the flow of tropical rivers. *Journal of Hydrology*, *200*(1–4), 24–39. https://doi.org/10.1016/S0022-1694(96)03340-9

Beggan, C. D., & Musur, M. A. (2019). Is the Madden–Julian Oscillation reliably detectable in Schumann Resonances? *Journal of Atmospheric and Solar-Terrestrial Physics*, *190*, 108–116. https://doi.org/10.1016/j.jastp.2019.05.009

Beirle, S., Koshak, W., Blakeslee, R., & Wagner, T. (2014). Global patterns of lightning properties derived by OTD and LIS. *Natural Hazards and Earth System Sciences*, *14*, 2715–2726. https://doi.org/10.5194/nhess-14-2715-2014

Blakeslee, R. J., Mach, D. M., Bateman, M. G., & Bailey, J. C. (2014). Seasonal variations in the lightning diurnal cycle and implications for the global electric circuit. *Atmospheric Research*, *135–136*, 228–243. https://doi.org/10.1016/j.atmosres.2012.09.023

Boccippio, D. J. (2001). Lightning scaling relations revisited. *Journal of the Atmospheric Sciences*, *59*(6), 1086–1104. https://doi.org/10.1175/1520-0469(2002)059<1086:LSRR>2.0.CO;2

Boccippio, D. J., Koshak, W., Blakeslee, R., Driscoll, K., Mach, D., Buechler, D., et al. (2000). The Optical Transient Detector (OTD): Instrument characteristics and cross-sensor validation. *Journal of Atmospheric and Oceanic Technology*, *17*(4), 441–458. https://doi.org/10.1175/1520-0426(2000)017<0441:TOTDOI>2.0.CO;2

Boldi, R., Williams, E., & Guha, A. (2018). Determination of the global-average charge moment of a lightning flash using Schumann resonances and the LIS/OTD lightning data. *Journal of Geophysical Research: Atmospheres*, *123*(1), 108–123. https://doi.org/10.1002/2017JD027050

Bór, J., Sátori, G., Barta, V., Szabóné-André, K., Szendrői, J., Wesztergom, V., et al. (2020). Measurements of atmospheric electricity in the Széchenyi István Geophysical Observatory, Hungary. *History of Geo- and Space Sciences*, *11*(1), 53–70. https://doi.org/10.5194/hgss-11-53-2020

Bozóki, T., Prácser, E., Sátori, G., Dálya, G., Kapás, K., & Takátsy, J. (2019). Modeling Schumann resonances with schupy. *Journal of Atmospheric and Solar-Terrestrial Physics*, *196*, 105144. https://doi.org/10.1016/j.jastp.2019.105144

Bradbury, T. (2000). *Meteorology and flight: A pilot's guide to weather*. London: A&C Black.

Cecil, D. J., Buechler, D. E., & Blakeslee, R. J. (2014). Gridded lightning climatology from TRMM-LIS and OTD: Dataset description. *Atmospheric Research*, *135*, 404–414. https://doi.org/10.1016/j.atmosres.2012.06.028

Cecil, D. J., Buechler, D. E., & Blakeslee, R. J. (2015). TRMM LIS climatology of thunderstorm occurrence and conditional lightning flash rates. *Journal of Climate*, *28*(16), 6536–6547. https://doi.org/10.1175/JCLI-D-15-0124.1

Chaudhari, H. S., Ranalkar, M. R., Kumkar, Y. V., Oh, J. H., & Singh, G. P. (2010). Study of lightning activity over Indian subcontinent. *Advances in Geosciences*, *16*, 121–131. https://doi.org/10.1142/9789812838100_0011

Chen, J., Dai, A., Zhang, Y., & Rasmussen, K. L. (2020). Changes in convective available potential energy and convective inhibition under global warming. *Journal of Climate*, *33*(6), 2025–2050. https://doi.org/10.1175/JCLI-D-19-0461.1

Chen, L., Li, T., Wang, B., & Wang, L. (2017). Formation mechanism for 2015/16 super El Niño. *Nature Scientific Report*, *7*, 2975. https://doi.org/10.1038/s41598-017-02926-3

Christian, H. J., Blakeslee, R. J., Boccippio, D. J., Boeck, W. L., Buechler, D. E., Driscoll, K.T., et al. (2003). Global frequency and distribution of lightning as observed from space by the optical transient detector. *Journal of Geophysical Research*, *108*(D1), ACL 4-1–ACL 4-15. https://doi.org/10.1029/2002JD002347

Chronis, T. G., Goodman, S. J., Cecil, D., Buechler, D., Robertson, F. J., & Pittman, J. (2008). Global lightning activity from the ENSO perspective. *Geophysical Research Letters*, *35*(19). https://doi.org/10.1029/2008GL034321

Clayton, M., & Polk, C. (1977). Diurnal variation and absolute intensity of worldwide lightning activity, September 1970 to May 1971. In H. Dolezalek & R. Reiter (Eds.), *Electrical Processes in Atmospheres* (pp. 440). Darmstadt, West Germany: Verlag.

Dong, L., & McPhaden, M. J. (2018). Unusually warm Indian Ocean sea surface temperatures help to arrest development of El Niño in 2014. *Nature Scientific Reports*, *8*, 2249. https://doi.org/10.1038/s41598-018-20294-4

Dowdy, A. J. (2016). Seasonal forecasting of lightning and thunderstorm activity in tropical and temperature regions of the world. *Nature Scientific Reports*, *6*, 20874. https://doi.org/10.1038/srep20874

Dyrda, M., Kulak, A., Mlynarczyk, J., Ostrowski, M., Kubisz, J., Michalec, A., & Nieckarz, Z. (2014). Application of the Schumann resonance spectral decomposition in characterizing the main African thunderstorm center. *Journal of Geophysical Research: Atmospheres*, *119*(23), 13338–13349. https://doi.org/10.1002/2014JD022613

Fan, J., Rosenfeld, D., Zhang, Y., Giangrande, S. E., Li, Z., Machado, L. A.T., et al. (2018). Substantial convection and precipitation enhancements by ultrafine aerosol particles. *Science*, *359*(6374), 411–418. https://doi.org/10.1126/science.aan8461

Goodman, S. J., Buechler, D. E., Knupp, K., Driscoll, K. T., & McCaul, E. W. (2000). The 1997–1998 El Niño event and related wintertime lightning variations in the southeastern United States. *Geophysical Research Letters*, *27*(4), 541–544. https://doi.org/10.1029/1999GL010808

Guha, A., Banik, T., Roy, R., & Kumar, B. (2017). The effect of El Nino and La Nina on lightning activity: Its relation with meteorological and cloud microphysical parameters. *Natural Hazards*, *85*, 403–424. https://doi.org/10.1007/s11069-016-2571-y

Halpert, M. S., & Ropelewski, C. F. (1992). Surface temperature patterns associated with the Southern Oscillation. *Journal of Climate*, *5*(6), 577–593. https://doi.org/10.1175/1520-0442(1992)005<0577:STPAWT>2.0.CO;2

Hamid, E. F., Kawasaki, Z. I., & Mardiana, R. (2001). Impact of the 1997–98 El Niño event on lightning activity over Indonesia. *Geophysical Research Letters*, *28*(1), 147–150. https://doi.org/10.1029/2000GL011374

Hansen, J., & Lebedeff, S. (1987). Global trends of measured surface air temperature. *Journal of Geophysical Research*, *92*(D11), 13345–13372. https://doi.org/10.1029/JD092iD11p13345

Hansen, J., Sato, M., Ruedy, R., Schmidt, G. A., Lo, K., & Persin, A. (2018). Global temperature in 2017. *NASA GISS website*. Retrieved from http://www.columbia.edu/~jeh1/mailings/2018/20180118_Temperature2017.pdf

Heckman, S., Williams, E., & Boldi, R. (1998). Total global lightning inferred from Schumann resonance measurements. *Journal of Geophysical Research*, *103*(D24), 31775–31779. https://doi.org/10.1029/98JD02648

Hu, J., Rosenfeld, D., Ryzhkov, A., Zrnic, D., Williams, E., Zhang, P., et al. (2019). Polarimetric radar convective cell tracking reveals large sensitivity of cloud precipitation and electrification properties to CCN. *Journal of Geophysical Research: Atmospheres*, *124*(22), 12194–12205. https://doi.org/10.1029/2019JD030857

Hutchins, M. L., Holzworth, R. H., Brundell, J. B., & Rodger, C. J. (2012). Relative detection efficiency of the World Wide Lightning Location Network. *Radio Science*, *47*(6). https://doi.org/10.1029/2012RS005049

Kandalgaonkar, S. S., Tinmaker, M. I. R., Kulkarni, J. R., & Nath, A. (2003). Diurnal variation of lightning activity over the Indian region. *Geophysical Research Letters*, *30*(20). https://doi.org/10.1029/2003GL018005

Kandalgaonkar, S. S., Tinmaker, M. I. R., Kulkarni, J. R., Nath, A., Kulkarni, M. K., & Trimbake, H. K. (2005). Spatio-temporal variability of lightning activity over the Indian region. *Journal of Geophysical Research*, *110*(D11). https://doi.org/10.1029/2004JD005631

Klein, S., Sodem, B. J., & Lau, N.-G. (1999). Remote sea surface temperature variations during ENSO: Evidence for a tropical atmospheric bridge. *Journal of Climate*, *12*(4), 917–932. https://doi.org/10.1175/1520-0442(1999)012<0917:RSSTVD>2.0.CO;2

Kulkarni, M. K., Revadekar, J. V., Verikoden, H., & Athale, S. (2015). Thunderstorm days and lightning activity in association with El Nino. *Vayu Mandal*, *41*, 39–43.

Kulkarni, M. N., & Siingh, D. (2014). The relation between lightning and cosmic rays during ENSO with and without IOD—A statistical study. *Atmospheric Research*, *143*, 129–141. https://doi.org/10.1016/j.atmosres.2014.02.010

Kumar, P. R., & Kamra, A. K. (2012). Variability of lightning activity in south/southeast Asia during 1997–98 and 2002–03 El Nino/La Nina events. *Atmospheric Research*, *118*, 84–102. https://doi.org/10.1016/j.atmosres.2012.06.004

Lim, Y.-K., Kovach, R. M., Pawson, S., & Vernieres, G. (2017). The 2015/2016 El Niño event in context of the MERRA-2 reanalysis: A comparison of the tropical Pacific with 1982/1983 and 1997/1998. *Journal of Climate*, *30*(13), 4819–4842. https://doi.org/10.1175/JCLI-D-16-0800.1

Märcz, F., & Sátori, G. (2005). Long-term changes in atmospheric electricity and the multivariate ENSO index. *Acta Geodaetica et Geophysica Hungarica*, *40*, 379–390. https://doi.org/10.1556/AGeod.40.2005.3-4.10

Märcz, F., Sátori, G., & Zieger, B. (1997). Variations in Schumann resonances and their relation to atmospheric electric parameters at Nagycenk station. *Annales Geophysicae*, *15*, 1604–1614. https://doi.org/10.1007/s00585-997-1604-y

Musur, M. A., & Beggan, C. D. (2019). Seasonal and Solar Cycle Variation of Schumann Resonance Intensity and Frequency at Eskdalemuir Observatory, UK. *Sun and Geosphere*, *14*(1). https://doi.org/10.31401/SunGeo.2019.01.11

Mushtak, V. C., & Williams, E. R. (2002). ELF propagation parameters for uniform models of the Earth-ionosphere waveguide. *Journal of Atmospheric and Solar-Terrestrial Physics*, *64*(18), 1989–2001. https://doi.org/10.1016/S1364-6826(02)00222-5

Nelson, P. H. (1967). *Ionospheric perturbations and Schumann resonance data*. Project NR-371-401. (PhD dissertation), Cambridge, MA:Geophysics Laboratory, Massachusetts Institute of Technology.

Nickolaenko, A. P., & Hayakawa, M. (2002). *Resonances in the Earth-ionosphere cavity*, Dordrecht, Netherlands: Kluwer Academic Publishers.

Nickolaenko, A. P., & Hayakawa, M. (2014). *Schumann Resonance for Tyros*. Japan: Springer. Retrieved from https://doi.org/10.1007/978-4-431-54358-9

Pawar, S. D., Lal, D. M., & Murugavel, P. (2011). Lightning characteristics over central India during Indian summer monsoon. *Atmospheric Research*, *106*, 44–49. https://doi.org/10.1016/j.atmosres.2011.11.007

Philander, S. G. (1990). *El Nino, La Nina, and the Southern Oscillation*, Cambridge, MA: Academic Press. https://www.elsevier.com/books/el-nino-la-nina-and-the-southern-oscillation/philander/978-0-12-553235-8

Prácser, E., Bozóki, T., Sátori, G., Williams, E., Guha, A., & Yu, H. (2019). Reconstruction of global lightning activity based on Schumann resonance measurements: Model description and synthetic tests. *Radio Science*, *54*(3), 254–267. https://doi.org/10.1029/2018RS006772

Price, C. (2016). ELF electromagnetic waves from lightning: The Schumann resonances. *Atmosphere*, *7*(9). https://doi.org/10.3390/atmos7090116

Price, C., & Federmesser, B. (2006). Lightning-rainfall relationships in Mediterranean winter thunderstorms. *Geophysical Research Letters*, *33*(7), L07813. https://doi.org/10.1029/2005GL024794

Romps, D. M. (2016). Clausius-Clapeyron scaling of CAPE for analytic solutions to RCE. *Journal of the Atmospheric Sciences*, *73*(9), 3719–3737. https://doi.org/10.1175/JAS-D-15-0327.1

Romps, D. M., Seeley, J. T., Vollaro, D., & Molinari, J. (2014). Projected increase in lightning strikes in the United States due to global warming. *Science*, *346*(6211), 851–854. https://doi.org/10.1126/science.1259100

Rosenfeld, D., Zheng, Y., Hashimshoni, E., Pöhlker, M. L., Jefferson, A., Pöhlker, C., et al. (2016). Satellite retrieval of cloud condensation nuclei concentrations by using clouds as CCN chambers. *Proceedings of the National Academy of Sciences*, *113*(21), 5828–5834. https://doi.org/10.1073/pnas.1514044113

Saha, U., Siingh, D., Kamra, A. K., Galanaki, E., Maitra, A., Singh, R. P., et al. (2017). On the association of lightning activity and projected change in climate over the Indian sub-continent. *Atmospheric Research*, *183*, 173–190. https://doi.org/10.1016/j.atmosres.2016.09.001

Said, R. K., Inan, U. S., & Cummins, K. L. (2010). Long-range lightning geolocation using a VLF radio atmospheric waveform bank. *Journal of Geophysical Research*, *115*(D23). https://doi.org/10.1029/2010JD013863

Sátori, G. (1996). Monitoring Schumann resonances-II. Daily and seasonal frequency variations. *Journal of Atmospheric and Terrestrial Physics*, *58*(13), 1483–1488. http://dx.doi.org/10.1016/0021-9169(95)00146-8

Sátori, G., Neska, M., Williams, E., & Szendrői, J. (2007). Signatures of the day-night asymmetry of the Earth-ionosphere cavity in high time resolution Schumann resonance records. *Radio Science*, *42*(2), RS2S10. https://doi.org/10.1029/2006RS003483

Sátori, G., Rycroft, M., Bencze, P., Märcz, F., Bór, J., Barta, V., et al. (2013). An overview of thunderstorm-related research on the atmospheric electric field, Schumann resonances, sprites, and the ionosphere at Sopron, Hungary. *Surveys in Geophysics*, *34*, 255–292. https://doi.org/10.1007/s10712-013-9222-6

Sátori, G., Szendrői, J., & Verő, J. (1996). Monitoring Schumann resonances—I. Methodology. *Journal of Atmospheric and Terrestrial Physics*, *58*(13), 1475–1481. https://doi.org/10.1016/0021-9169(95)00145-X

Sátori, G., Williams, E., & Lemperger, I. (2009). Variability of global lightning activity on the ENSO time scale. *Atmospheric Research*, *91*(2-4), 500–507. http://dx.doi.org/10.1016/j.atmosres.2008.06.014

Sátori, G., Williams, E., Price, C., Boldi, R., Koloskov, A., Yampolski, Y., et al. (2016). Effects of energetic solar emissions on the Earth-ionosphere cavity of Schumann resonances. *Surveys in Geophysics*, *37*, 757–789. https://doi.org/10.1007/s10712-016-9369-z

Sátori, G., & Zieger, B. (1999). El Niño related meridional oscillation of global lightning activity. *Geophysical Research Letters*, *26*(10), 1365–1368. https://doi.org/10.1029/1999GL900264

Schumann, W. O. (1952). Über die strahlungslosen Eigenschwingungen einer leitenden Kugel, die von einer Luftschicht und einer Ionosphärenhülle umgeben ist. *Zeitschrift und Naturfirschung*, *7*(2), 149–154. https://doi.org/10.1515/zna-1952-0202

Siingh, D., Dharmaraj, T., Kumar, P. R., Singh, R., Kumar, S., Chunthalu, G. R., et al. (2017). Variability of lightning, convective rain and solar activity study over south/southeast Asia during ENSO episodes for the period 1998-2010. *Journal of Indian Geophysical Union*, *21*(5), 401–414.

Stolz, D. C., Rutledge, S. R., Pierce, J., & van den Heever, S. (2017). A global lightning parameterization based on statistical relationships between environmental factors, aerosols, and convective clouds in the TRMM climatology. *Journal of Geophysical Research: Atmospheres*, *122*(14), 7461–7492. https://doi.org/10.1002/2016JD026220

Thornton, J. A., Virts, K. S., Holzworth, R. H., & Mitchell, T. P. (2017). Lightning enhancement over major shipping lanes. *Geophysical Research Letters*, *44*(17), 9102–9111. https://doi.org/10.1002/2017GL074982

Tinmaker, M. I. R., Aslam, M. Y., Ghude, S. D., & Chate, D. M. (2017). Lightning activity with rainfall during El Nino and La Nina events over India. *Theoretical and Applied Climatology*, *130*, 391–400. https://doi.org/10.1007/s00704-016-1883-x

Trenberth, K. E., Caron, J. M., Stepaniak, D. P., & Worley, S. (2002). Evolution of El Nino–Southern Oscillation and global atmospheric surface temperatures. *Journal of Geophysical Research*, *107*(D8), AAC 5-1–AAC 5-17. https://doi.org/10.1029/2000JD000298

Wait, J. R. (1970). *Electromagnetic Waves in Stratified Media*. New York, Oxford: The Institute of Electrical and Electronics Engineers Inc., University Press Oxford.

Wang, M., Williams, E., Rosenfeld, D., Venevsky, S., Guha, A., Wu, Y.-J., et al. (2018a). Possible role of cloud condensation nuclei (CCN) in Africa's dominance of the AC global circuit. *Fall Meeting of the American Geophysical Union, Washington, DC, December 14-18*.

Wang, Q., Li, Z., Guo, J., Zhao, C., & Cribb, M. (2018b). The climate impact of aerosols on lightning: Is it detectable from long-term aerosol and meteorological data? *Atmospheric Chemistry and Physics*, *18*, 12797–12816. https://doi.org/10.5194/acp-18-12797-2018

Williams, E. R. (1992). The Schumann resonance: A global tropical thermometer. *Science*, *256*(5060), 1184–1187. https://doi.org/10.1126/science.256.5060.1184

Williams, E. R. (1994). Global circuit response to seasonal variations in global surface air temperature. *Monthly Weather Review*, *122*(8), 1917–1929. https://doi.org/10.1175/1520-0493(1994)122<1917:GCRTSV>2.0.CO;2

Williams, E. R. (2012). *Franklin lecture: Lightning and Climate*. San Francisco: AGU Fall Meeting. Retrieved from https://abstractsearch.agu.org/meetings/2012/FM/AE31A-01.html

Williams, E. R. (2020). Chapter 2: "Lightning and Climate Change" Chapter 2 in book. In A. Piantini (Ed.), *Lightning Interaction with Power Systems*. Stevenage: UK: The Institution of Engineering and Technology

Williams, E., Guha, A., Boldi, R., Christian, H., & Buechler, D. (2019). Global lightning activity and the hiatus in global warming. *Journal of Atmospheric and Terrestrial Physics*, *189*, 27–34. https://doi.org/10.1016/j.jastp.2019.03.011

Williams, E. R., & Heckman, S. J. (1993). The local diurnal variation of cloud electrification and the global diurnal variation of the negative charge on the earth. *Journal of Geophysical Research*, *98*(D3), 5221–5234. https://doi.org/10.1029/92JD02642

Williams, E. R., & Mareev, E. A. (2014). Recent progress on the global electrical circuit. *Atmospheric Research*, *135–136*, 208–227. https://doi.org/10.1016/j.atmosres.2013.05.015

Williams, E. R., Mushtak, V. C., Rosenfeld, D., Goodman, S. J., & Boccippio, D. J. (2005). Thermodynamic conditions favorable to superlative thunderstorm updraft, mixed phase microphysics and lightning flash rate. *Atmospheric Research*, *76*(1–4), 288–306. https://doi.org/10.1016/j.atmosres.2004.11.009

Williams, E. R., & Renno, N. O. (1993). An analysis of the conditional instability of the tropical atmosphere. *Monthly Weather Review*, *121*(1), 21–36. https://doi.org/10.1175/1520-0493(1993)121<0021:AAOTCI>2.0.CO;2

Williams, E. R., Rosenfeld, D., Madden, N., Gerlach, J., Gears, N., Atkinson, L., et al. (2002). Contrasting convective regimes over the Amazon: Implications for cloud electrification. *Journal of Geophysical Research*, *107*(D20), LBA 50-1–LBA 50-19. LBA Special Issue. https://doi.org/10.1029/2001JD000380

Williams, E. R., Rothkin, K., Stevenson, D., & Boccippio, D. (2000). Global lightning variations caused by changes in thunderstorm flash rate and by changes in the number of thunderstorms. *Journal of Applied Meteorology and Climatology*, *39*(12), 2223–2230.TRMM Special Issue. https://doi.org/10.1175/1520-0450(2001)040<2223:GLVCBC>2.0.CO;2

Williams, E., & Stanfill, S. (2002). The physical origin of the land-ocean contrast in lightning activity. *Comptes Rendus Physique*, *3*(10), 1277–1292. https://doi.org/10.1016/S1631-0705(02)01407-X

Wu, Y. J., Chen, A. B., Hsu, H. H., Chou, J. K., Chang, S. C., Lee, L. J., et al. (2012). Occurrence of elves and lightning during El Nino and La Nina. *Geophysical Research Letters*, *39*(3). https://doi.org/10.1029/2011GL049831

Wu, Y. J., Hsu, R. R., Chen, A. B. C., Su, H. T., Chang, S. C., Chou, J. K., et al. (2017). Revisiting oceanic elves and lightning occurrence rate during El Niño and La Nina episodes in a 10-year time frame. *Terrestrial, Atmospheric and Oceanic Sciences*, *28*(4). https://doi.org/10.3319/TAO.2016.07.28.01

Yoshida, S., Morimoto, T., Ushio, T., & Kawasaki, Z. (2007). ENSO and convective activities in Southeast Asia and western Pacific. *Geophysical Research Letters*, *34*(21). https://doi.org/10.1029/2007GL030758

Yuan, T., Di, Y., & Qie, K. (2016). Variability of lightning flash and thunderstorm over East/Southeast Asia on the ENSO time scales. *Atmospheric Research*, *169*(A), 377–390. https://doi.org/10.1016/j.atmosres.2015.10.022